JPET Fast Forward. Published on November 17, 2020 as DOI: 10.1124/jpet.120.000065
This article has not been copyedited and formatted. The final version may differ from this version.

1. TITLE PAGE

Pharmacological Actions of Carbamate Insecticides at Mammalian Melatonin Receptors

Grant C. Glatfelter[1,2], Anthony J. Jones[1], Rajendram V. Rajnarayanan[3], and Margarita L. Dubocovich[4]

Department of Pharmacology & Toxicology (G.C.G., A.J.J., R.V.R., M.L.D.), Interdepartmental Neuroscience Program (A.J.J., M.L.D.), Jacobs School of Medicine and Biomedical Sciences - University at Buffalo, Buffalo, NY 14203.

JPET Fast Forward. Published on November 17, 2020 as DOI: 10.1124/jpet.120.000065
This article has not been copyedited and formatted. The final version may differ from this version.

2. RUNNING TITLE PAGE

Running Title: Pharmacology of Carbamate Insecticides at Melatonin Receptors

Corresponding Author:

Margarita L. Dubocovich, Ph.D.

Department of Pharmacology and Toxicology

Jacobs School of Medicine and Biomedical Sciences

955 Main Street (Rm 3102)

University at Buffalo (SUNY)

Buffalo, NY 14203

Phone: 1-716-829-3048; Fax: 1-716-829-2801; Email: mdubo@buffalo.edu

# of text pages = 28 (intro - discussion), 70 total

# of tables = 3 + 5 supplemental

# of figures = 9 + 5 supplemental

# of references = 97

# of words in Abstract = 235

# of words in Introduction = ~700

# of words in Discussion = ~1604

Non- Standard Abbreviations

AChE: Acetylcholinesterase

CHO: Chinese Hamster Ovary Cells

CT: Circadian Time (Onset of running wheel activity in constant conditions = CT 12)

hMT_1: Human Melatonin Receptor 1

hMT_2: Human Melatonin Receptor 2

KO: Knockout

mMT_1: Mouse Melatonin Receptor 1

mMT_2: Mouse Melatonin Receptor 2

JPET Fast Forward. Published on November 17, 2020 as DOI: 10.1124/jpet.120.000065
This article has not been copyedited and formatted. The final version may differ from this version.

MT_1: Melatonin Receptor 1

MT_2: Melatonin Receptor 2

PT: Pars Tuberalis

PVT: Paraventricular Nucleus of the Thalamus

RW: Running Wheel

SCN: Suprachiasmatic Nucleus

VEH: Vehicle

WT: Wild-Type

ZT: Zeitgeber Time (Lights on = ZT 0 under a light/dark cycle)

Recommended section assignment for JPET:

1) Neuropharmacology

2) Toxicology

JPET Fast Forward. Published on November 17, 2020 as DOI: 10.1124/jpet.120.000065
This article has not been copyedited and formatted. The final version may differ from this version.

3. ABSTRACT

Integrated *in silico* chemical clustering and melatonin receptor molecular modeling combined with *in vitro* 2-[^{125}I]-iodomelatonin competition binding were used to identify carbamate insecticides with affinity for hMT_1 and hMT_2 melatonin receptors. Saturation and kinetic binding studies with 2-[^{125}I]-iodomelatonin revealed lead carbamates (carbaryl, fenobucarb, bendiocarb, carbofuran) to be orthosteric ligands with antagonist apparent efficacy at hMT_1 and agonist apparent efficacy at hMT_2 melatonin receptors. Further using quantitative receptor autoradiography in coronal brain slices from C3H/HeN mice, carbaryl, fenobucarb, and bendiocarb competed for 2-[^{125}I]-iodomelatonin binding in the suprachiasmatic nucleus (SCN), thalamic paraventricular nucleus (PVT), and pars tuberalis (PT) with affinities similar to those determined for the hMT_1 receptor. Carbaryl (10 mg/kg i.p.) administered *in vivo* also competed *ex vivo* for 2-[^{125}I]-iodomelatonin binding to the SCN, PVT, and PT demonstrating the ability to reach brain melatonin receptors in C3H/HeN mice. Further, the same dose of carbaryl given to C3H/HeN mice for 3 consecutive days approximately 2 hours before running wheel activity onset (CT 10) in constant dark phase-advanced circadian activity rhythms (mean = 0.91 h) similar to melatonin (mean = 1.12 h) when compared to vehicle (mean = 0.04 h). Carbaryl-mediated phase shift of overt circadian activity rhythm onset is likely mediated via interactions with SCN melatonin receptors. Based on the pharmacological actions of carbaryl and other carbamate insecticides at melatonin receptors, exposure may modulate time-of-day information conveyed to the master biological clock relevant to adverse health outcomes.

JPET Fast Forward. Published on November 17, 2020 as DOI: 10.1124/jpet.120.000065
This article has not been copyedited and formatted. The final version may differ from this version.

4. Significance Statement (Max 80 words; currently 74 words 2 sentences)

In silico chemical clustering and molecular modeling in conjunction with *in vitro* bioassays identified several carbamate insecticides (i.e., carbaryl, carbofuran, fenobucarb, bendiocarb) as pharmacologically active orthosteric MT_1 and MT_2 receptor ligands. This work further demonstrated that carbaryl competes for melatonin receptor binding in the master biological clock (suprachiasmatic nucleus) and phase advances overt circadian activity rhythms in C3H/HeN mice, supporting the relevance of circadian effects when interpreting toxicological findings related to carbamate insecticide exposure.

JPET Fast Forward. Published on November 17, 2020 as DOI: 10.1124/jpet.120.000065
This article has not been copyedited and formatted. The final version may differ from this version.

5. VISUAL ABSTRACT (separate file)

JPET Fast Forward. Published on November 17, 2020 as DOI: 10.1124/jpet.120.000065
This article has not been copyedited and formatted. The final version may differ from this version.

6. INTRODUCTION

Melatonin modulates MT_1 and MT_2 melatonin G protein-coupled receptor (GPCR) signaling to regulate circadian phase and amplitude of physiological processes through action at brain (suprachiasmatic nucleus or SCN) and peripheral (pancreas) receptors (Bothorel et al., 2002; Dubocovich and Markowska, 2005; Dubocovich et al., 2010; Peschke et al., 2013; Jockers et al., 2016; Liu et al., 2016; Karamitri and Jockers, 2019). Notably, the “hormone of darkness” and its receptors regulate circadian rhythms, metabolism, mood as well as behavior, the cardiovascular and the immune systems, as well as other key physiological functions (Dubocovich et al., 2010; Jockers et al., 2016; Liu et al., 2016). Circadian misalignments, or out-of-phase rhythms, are linked to increased risk for obesity, diabetes, cancer, cardiovascular disease, as well as sleep and psychiatric disorders (Baron and Reid, 2014). It follows that exposure to environmental melatonin mimics, like recently reported carbamate insecticides (Popovska-Gorevski et al., 2017), could disrupt melatonin system signaling resulting in disturbed physiological function and exacerbation of disease pathologies.

Current initiatives aiming to identify risks of environmental chemical exposure (Tox21; (Kavlock et al., 2009; Schmidt, 2009; Tice et al., 2013) do not have measures to assess the ability of target compounds to interact with melatonin receptors and alter associated circadian or other biological functions. Our team is optimizing an integrated *in silico* to *in vivo* pipeline approach to identify environmental circadian disruptors, specifically those that target melatonin receptors. In collaboration with other teams, our group recently utilized a similar strategy that was successful in identifying novel MT_1 and MT_2 leads (Stein et al., 2020). Further, we also demonstrated that two carbamate

JPET Fast Forward. Published on November 17, 2020 as DOI: 10.1124/jpet.120.000065
This article has not been copyedited and formatted. The final version may differ from this version.

insecticides, structurally similar to melatonin, inhibited 2-[^{125}I]-iodomelatonin binding to recombinant hMT_1 and hMT_2 melatonin receptors (Popovska-Gorevski et al., 2017), thus prompting further investigations into the pharmacological actions of these compounds at melatonin receptors mediating time-of-day messages in target tissues (Dubocovich, 2007; Liu et al., 2016).

Carbamate insecticides, used industrially and domestically, are acutely toxic to insects and mammals due to reversible inhibition of acetylcholinesterase (AChE) and other esterases (Casida, 1963; Ecobichon, 2001; Moser et al., 2015b; Casida and Bryant, 2017). Use of carbaryl (1-naphthyl methylcarbamate) and other carbamates (e.g., aldicarb, bendiocarb, carbofuran, fenobucarb, fenoxycarb, methomyl, oxamyl) in agriculture as well as at home results in exposure for humans and other mammals evidenced by trace amounts in foods, soil, as well as surface water and groundwater (Gunaskara et al., 2008; Clark-Reyna et al., 2016). Environmental and occupational exposure to carbamate insecticides has been associated with various symptoms (Whorton et al., 1979; Wyrobek et al., 1981; Meeker et al., 2004; Xia et al., 2005; Ali et al., 2015; Manyilizu and Mdegela, 2015; Bini Dhouib et al., 2016; Meyer et al., 2017) and disease pathologies (Zheng et al., 2001; Mahajan et al., 2007; Saldana et al., 2007; Montgomery et al., 2008; Slager et al., 2010; Lebov et al., 2015; Baumert et al., 2018; Patel et al., 2018; Patel and Sangeeta, 2019) related to toxicity, thought to be caused by canonical actions of carbamate insecticides on the cholinergic system, to inhibit AChE. However, recent epidemiological evidence in US farmers showed that out of 63 pesticides tested (most of which act primarily on AChE), only exposure to carbamate insecticides (carbofuran and carbaryl) directly associated with sleep apnea suggesting

JPET Fast Forward. Published on November 17, 2020 as DOI: 10.1124/jpet.120.000065
This article has not been copyedited and formatted. The final version may differ from this version.

an ancillary mechanism of disease pathology that could involve interaction with melatonin receptors (Zirlik et al., 2013; Baumert et al., 2018). Carbamate insecticides could, therefore, influence the pathology of sleep as well as oncological, metabolic, and psychiatric disorders through pharmacological actions at melatonin receptors independent of or in addition to canonical actions at AChE.

Both increased (Tuomi et al., 2016) and decreased (Sulkava et al., 2016; Sulkava et al., 2018) melatonin receptor signaling, presumably at inappropriate times of day, is associated with increased circadian disruption-related disease risk (Schroeder and Colwell, 2013). Disruption of GPCR signaling through allosteric binding of endogenous ligands such as ions, amino acids, peptides, lipids, and autoantibodies have also been implicated in disease pathology (van der Westhuizen et al., 2015). Most, if not all, GPCRs possess allosteric binding pockets and while functional extracellular allosteric pockets on melatonin receptors have not yet been described, recent structural data supports this possibility (Stauch et al., 2020).

Our overall hypothesis was that carbamate insecticides with high structural similarity to melatonin would interact with melatonin receptors at orthosteric sites to alter signaling leading to alterations of circadian phase. We first utilized large library pharmacoinformatic screening tools and chemical similarity cluster analyses to identify carbamate insecticides with the highest likelihood of interacting with melatonin receptors. Pharmacological interactions between common carbamate insecticides with hMT_1 and hMT_2 melatonin receptors, structure-activity relationships, as well as binding mechanism(s) via docking to *in silico* receptor models, and *in vitro* competition for 2-[^{125}I]-iodomelatonin binding were then determined to identify binding mechanisms via

JPET Fast Forward. Published on November 17, 2020 as DOI: 10.1124/jpet.120.000065
This article has not been copyedited and formatted. The final version may differ from this version.

orthosteric and/or allosteric sites as well as apparent efficacy. We next tested the ability of the most potent carbamates (carbaryl, bendiocarb, fenobucarb) to bind to melatonin receptors in target brain areas (SCN, PVT, PT) via quantitative receptor autoradiography *in vitro* as well as the ability of carbaryl to reach brain melatonin receptors *in vivo* via *ex vivo* 2-[^{125}I]-iodomelatonin binding using C3H/HeN mice. Lastly, we tested the ability of carbaryl to alter circadian phase in C3H/HeN mice when given at subjective dusk to determine whether carbamate exposure could modulate circadian biology in a translational mouse model.

JPET Fast Forward. Published on November 17, 2020 as DOI: 10.1124/jpet.120.000065
This article has not been copyedited and formatted. The final version may differ from this version.

7. MATERIALS AND METHODS

Pharmacoinformatics and Chemical Similarity Clustering.

A series of carbamate-like structures were identified using a fragment-based query on Chem2Risk, a large pharmacoinformatics knowledgebase containing more than 4 million environmental chemicals (Popovska-Gorevski et al., 2017). Chemical clustering was performed using computed 2D and 3D Tanimoto chemical similarity indices as described earlier (Popovska-Gorevski et al., 2017).

Molecular Docking of Environmental Melatonin Ligands.

Two- and three- dimensional chemical structures of melatonin and all insecticides used in this study were generated using Marvin Sketch (ChemAxon, USA). Protein structures of MT_1 and MT_2 melatonin receptors were generated as described in Popovska-Gorevski et al. (2017). The SYBYL X software (Cerata USA, Inc., Princeton, NJ) package was used to prepare the protein and ligands for molecular docking experiments. The putative binding pockets for MT_1 (inclusive of residues H195, S110, and S112) and for MT_2 (inclusive of residues N175, H208, N268, and Y298) were inferred from mutagenesis data (See Tables 2 and 3 (Dubocovich et al., 2010). Surflex-Dock (SYBYL, Cerata USA, Inc., Princeton, NJ) and VINA (Autodock, Molecular Docking, The Scripps Research Institute) were employed to dock select environmental carbamates against human melatonin receptor models. Ligands were rendered flexible in surflex docking routine, multiple conformations (docked poses) were generated and scored using surflex score (CScore; arbitrary units) which includes a combination of Dock-score, Gold-score, PMF-score, and CHEM-score. Twenty conformations for each

JPET Fast Forward. Published on November 17, 2020 as DOI: 10.1124/jpet.120.000065
This article has not been copyedited and formatted. The final version may differ from this version.

protein-ligand docking experiment were retrieved and top docked poses were selected based on the orientation of the test ligand with respect to the reference ligand and its docking score. Recently, high-resolution crystal structures of MT_1 in complex with agomelatine (6ME5), ramelteon (6ME2), 2-phenylmelatonin (6ME3) and 2-iodomelatonin (6ME4) and MT_2 melatonin receptor in complex with ramelteon (6ME9) and 2-phenylmelatonin (6ME6) were released (Johansson et al., 2019; Stauch et al., 2019). Carbamate insecticides were docked into the binding pockets of these newly released melatonin receptors 6ME2-9 using the protocol as described above.

Cell Culture and Harvesting.

The derivation of CHO cells stably expressing FLAG-tagged recombinant human MT_1 or MT_2 melatonin receptors (CHO-hMT_1 and CHO-hMT_2) was described previously (Gerdin et al., 2003). CHO cells were cultured in Ham's F12 media supplemented with 10% fetal calf serum, 1% HEPES, and 1% penicillin (10,000 IU/mL)/streptomycin (10,000 µg/mL) in 5% CO2 at 37 °C and harvested as described previously (Popovska-Gorevski et al., 2017). Cell lines were determined to be mycoplasma-free using the LookOut® Mycoplasma PCR Detection Kit (Sigma-Aldrich). Products for cell culture were obtained from VWR International (Pittsburgh, PA, USA). All other chemicals were reagent grade.

2-[^{125}I]-Iodomelatonin Binding Assays.

CHO-hMT_1 and CHO-hMT_2 cell pellets were suspended, homogenized, and washed twice by centrifugation (12,000 rpm) in Tris-HCl buffer. Competition binding

JPET Fast Forward. Published on November 17, 2020 as DOI: 10.1124/jpet.120.000065
This article has not been copyedited and formatted. The final version may differ from this version.

studies for selected compounds were conducted as previously described (Popovska-Gorevski et al., 2017) in active conformation buffer (50 mM Tris-HCl, 10 mM $MgCl_2$, pH 7.4 at 25 °C) or in resting conformation buffer (50 mM Tris-HCl, 10 mM $MgCl_2$, 100 μM GTP, 1 mM EDTA.Na_2, 150 mM NaCl, pH 7.4 at 25 °C). Briefly, CHO-hMT_1 or CHO-hMT_2 cell membrane suspensions [9 (7 to 11) and 14 (11 to 17) μg protein/assay (95% CI), respectively] were incubated with 2-[^{125}I]-iodomelatonin [75 (66 to 83) pM] in the absence and presence of carbamate insecticides (10 nM to 10 mM) or vehicle at 25 ºC (1 h for CHO-hMT_1; 1.5 h for CHO-hMT_2). Final concentrations of ethanol in assays for concentrations of 1 mM or 0.1 mM did not exceed 4%. Additional equilibrium binding assays were performed using CHO-hMT_1 or CHO-hMT_2 cell membranes in active conformation buffer with titrated concentrations of 2-[^{125}I]-iodomelatonin (50-1400 pM) in the absence and presence of melatonin, luzindole, or carbaryl (10 pM to 1 mM) at 25 ºC (1 h for CHO-hMT_1; 1.5 h for CHO-hMT_2). Further titration assays for luzindole and carbaryl binding to CHO-hMT_1 membranes were conducted in resting buffer to prevent high-affinity 2-[^{125}I]-iodomelatonin binding to the G protein-coupled form of the receptor. For allosteric screening dissociation assays, 2-[^{125}I]-iodomelatonin (75 ± 4 pM) binding to membranes in resting buffer was allowed to reach equilibrium at 25 ºC (1 h for CHO-hMT_1; 1.5 h for CHO-hMT_2) then dissociation was initiated using 10 μM melatonin in the absence or presence of vehicle, luzindole, or carbamate insecticide (100 μM). After 1 hour for competition binding studies or at various time points (1-40 min) for dissociation assays, incubation was terminated by vacuum filtration through glass microfiber filters pre-soaked in 0.5% polyethyleneimine. Filters were then washed twice and counts per minute (cpm) were measured by a gamma-counter.

JPET Fast Forward. Published on November 17, 2020 as DOI: 10.1124/jpet.120.000065
This article has not been copyedited and formatted. The final version may differ from this version.

Animals.

Male C3H/HeN wild type (WT) mice from our colony and C3H/HeN mice homozygous for the MT_2 melatonin receptor gene deletion (MT_2KO) originally donated by Dr. Steven Reppert (Worcester, MA) were bred and maintained in the Laboratory of Animal Facility at University at Buffalo as previously described (Hutchinson et al., 2012). Mice were housed in a 14/10 light/dark cycle (ZT: Zeitgeber Time; ZT 0: lights on 5 AM) in temperature (22 ± 1 °C) and humidity controlled environments with *ad libitum* access to food (Harlan Teklad 2018sx) and water. Light levels were 200-300 lux at the level of the cage and mice were housed with corncob bedding in polycarbonate translucent cages without running wheels (RW; 30 x 19 cm) or with RW (33 x 15 cm: Phenome Technologies). All procedures were approved by the University at Buffalo Institutional Animal Care and Use Committee and followed National Institute of Health guidelines. All mice for experiments in this manuscript were randomly assigned to respective treatment conditions.

Coronal Brain Slice Preparation

Preparation of coronal brain slices was adapted from previously described methods (Siuciak et al., 1990; Benloucif et al., 1997). WT and MT_2KO C3H/HeN mice were euthanized by decapitation between ZT 8 and ZT 10. Mouse brains were dissected, flash-frozen using 2-methylbutane, and stored at -80 °C until sectioning. Adjacent coronal brain sections (20 µm) were cut at -20 °C using a cryostat (Leica CM3050S) encompassing regions of interest (i.e., SCN, PVT, PT). Sections were

JPET Fast Forward. Published on November 17, 2020 as DOI: 10.1124/jpet.120.000065
This article has not been copyedited and formatted. The final version may differ from this version.

immediately thaw mounted onto silane coated slides (Azer Scientific) and stored at -20 °C until further use.

In vitro Quantitative Receptor Autoradiography.

Receptor autoradiography methods were as previously described (Siuciak et al., 1990; Dubocovich et al., 1998). Each C3H/HeN mouse brain provided two sets of six separate slides containing 6-8 adjacent sections containing SCN and PVT or PT brain regions. Slide-mounted sections stored at -20 °C were air-dried for 15 minutes at room temperature before incubation with various treatments during a 1-hour incubation period. Treatments all contained 2-[^{125}I]-iodomelatonin (75 pM) prepared in Tris-Ca buffer (50 mM Tris-HCl and 4 mM CaCl, pH 7.4) in the absence (total binding) or presence of varying concentrations (1, 10, 100 µM) of carbaryl, bendiocarb, fenobucarb, melatonin (1 µM, positive control, and non-specific binding), or vehicle (Tris-Ca Buffer 7.7% ethanol). Post incubation, slides were rinsed twice with Tris-Ca buffer (10 minutes) and rapidly rinsed in deionized water (all solutions ice cold) before being air-dried at room temperature under dim light. Slides were then pressed to x-ray film (Kodak) for 14 days before being developed (Kodak D19). Optical densities (OD) from autoradiograms in brain regions of interest were then measured with Image J analysis software (NIH), transformed using ^{14}C standard slides calibrated for use with ^{125}I (Miller and Zahniser, 1987), and used to determine competition for 2-[^{125}I]-iodomelatonin binding across treatments (Miller and Zahniser, 1987; Masana et al., 2000). Data points are composed of averages of raw OD values obtained in 2-3 adjacent sections/treatment/brain region divided by the total density (treated OD value / total non-treated OD value x 100) to

JPET Fast Forward. Published on November 17, 2020 as DOI: 10.1124/jpet.120.000065
This article has not been copyedited and formatted. The final version may differ from this version.

yield % total binding for each set of adjacent sections for individual mouse brains. Vehicle-treated control groups contained a minimum of *n* = 2 - 4 while experimental treatment groups contained *n* = 4 - 7 depending on the number of viable sections for each brain.

Ex vivo Quantitative Receptor Autoradiography.

Based on methods described in Beresford et al. (1998), C3H/HeN mice were treated *in vivo* with vehicle (corn oil i.p.) or carbaryl (10 mg/kg i.p.) at ZT 8. Treatments were administered at ZT 8 to avoid influence of endogenous melatonin produced in C3H/HeN mice (Masana et al., 2000). Carbaryl dose (10 mg/kg) and route (i.p.) of administration were selected based on lack of known AChE inhibition-mediated toxic and/or behavioral effects at this dose as well as reported brain biodistribution (Declume and Benard, 1977; Albright and Simmel, 1979; Ruppert et al., 1983a; Moser et al., 1988; Moser, 1995; Krolski et al., 2003; Moser et al., 2012; Wang et al., 2014; Moser et al., 2015a; Moser et al., 2015b). Mice were euthanized by decapitation at 0, 30, 60, 120, or 240 minutes post-injection. Brains were dissected immediately and prepared for quantitative autoradiography as described (Siuciak et al., 1990; Masana et al., 2000). Brain sections from mice treated *in vivo* with vehicle or carbaryl were then labeled *in vitro* and processed for quantitative receptor autoradiography with 2-[^{125}I]-iodomelatonin (50 pM) prepared in Tris-Ca buffer (50 mM Tris-HCl and 4 mM CaCl, pH 7.4) in the absence (total binding) or presence of melatonin (1 µM) (non-specific binding) used as positive control. Specific binding was defined by subtracting non-specific binding values from total binding for each brain slice. Each value represents data from 2 - 3 adjacent

JPET Fast Forward. Published on November 17, 2020 as DOI: 10.1124/jpet.120.000065
This article has not been copyedited and formatted. The final version may differ from this version.

slices from a single mouse brain. Final *n* values for carbaryl treated mice ranged from 3 - 6 (SCN, PVT) or 2 - 3 (PT) due to the number of viable slices in each brain assessed. Values for vehicle controls euthanized 0 (*n* = 6) or 240 (*n* = 4) post-injection were pooled for comparisons to carbaryl treatment across time (total *n* = 10). Data represent two individual experiments used to compare competition for radioligand binding *ex vivo* across treatment time points.

Carbaryl-Mediated Phase Shift of Circadian Rhythm of Running Wheel Activity Onset.

Methods are previously described in Benloucif and Dubocovich (1996); Dubocovich et al. (1998), and Dubocovich et al. (2005). Briefly, male C3H/HeN mice were housed in constant darkness for 2 weeks before treatment to establish stable free-running circadian rhythms of RW activity. Vehicle (saline/15% ethanol), carbaryl (10 mg/kg i.p.), or melatonin (3 mg/kg, s.c.) treatments were given for 3 consecutive days at approximately circadian time 10 (CT: CT 12 = onset of running wheel activity; CT 10 = 2 hours onset of circadian rhythm of wheel-running activity). Times of treatments were determined from actograms by predicted onset of running wheel activity for each mouse based on stable free-running activity rhythm onsets for 7-12 days before treatments and were centered around CT 10, occurring from CT 9 - 11 (average time of injections was CT 10.1 - 10.2 respectively for days 1 - 3). Injections and animal care in constant dark were done by dim red light (< 5 lux) to avoid influence of light on circadian running wheel activity rhythms (Benloucif and Dubocovich, 1996; Benloucif et al., 1999). The shift in time of post-treatment activity rhythm onset fits of 7-12 days were compared to pre-treatment onset fits on the first day after treatment to determine phase shift values.

JPET Fast Forward. Published on November 17, 2020 as DOI: 10.1124/jpet.120.000065
This article has not been copyedited and formatted. The final version may differ from this version.

An earlier onset in the post-treatment onsets relative to pre-treatment onsets is considered a phase advance while the opposite would be a phase delay in activity rhythms. Actograms were analyzed blind to treatment and were excluded before analyses if mice displayed tau changes greater than 0.3, low activity, or if 2/3 injections occurred outside the target window. Only 1 mouse was excluded based on the aforementioned criteria from the carbaryl treatment group for having 2/3 injections fall outside the acceptable time window. Negative (vehicle: *n* = 7) and positive (melatonin: *n* = 4) controls were compared to carbaryl treated mice (*n* = 12) to assess effects of treatment on magnitude of phase changes post-treatment. Data were replicated in 2 separate experiments (experiment 1: *n* = 3 vehicle, *n* = 5 carbaryl; experiment 2: *n* = 4 vehicle, *n* = 8 carbaryl, *n* = 4 melatonin) pooled together for statistical analysis (total *n* = 24 individual mice).

Reagents

2-[^{125}I]-iodomelatonin (SA: 2,200 ci, 81.4TBq/mmol) was purchased from Perkin Elmer (Shelton, CT, USA). Guanosine 5'-triphosphate sodium salt hydrate (GTP), melatonin, aldicarb, bendiocarb, carbaryl, carbofuran, fenobucarb, fenoxycarb, methomyl, oxamyl, and corn oil were obtained from Sigma-Aldrich (St. Louis, MO, USA). Luzindole was purchased from Tocris (Minneapolis, MN, USA).

Compound and Drug Preparation

For in vitro experiments melatonin and luzindole (13 mM stock solutions) as well as aldicarb, bendiocarb, carbaryl, and fenobucarb (130 mM stock solutions) were

JPET Fast Forward. Published on November 17, 2020 as DOI: 10.1124/jpet.120.000065
This article has not been copyedited and formatted. The final version may differ from this version.

prepared in ethanol and subsequently diluted 1/10 in 50% ethanol/50% Tris-HCl buffer (50 mM, 10mM $MgCl_2$, pH 7.4 at 25 °C). Fenoxycarb (130 mM and 13 mM) were made in 100% ethanol and next diluted 1/10 in 50% ethanol/50% Tris-HCl buffer. Methomyl and oxamyl (130 mM stock solutions) were dissolved in water. All subsequent dilutions were performed in Tris-HCl buffer.

For *ex vivo* binding studies, carbaryl was dissolved in corn oil (1 mg/ml) at 37 ºC and administered at 0.01 mL/g mouse body weight for a dose of 10 mg/kg (i.p.). For phase shift experiments carbaryl was dissolved in 100% EtOH and diluted in sterile saline to 1mg/ml in 15% ethanol under continuous sonication and administered at 0.01 mL/g mouse body weight for a dose of 10 mg/kg (i.p.). Melatonin (0.9 mg/ml) was dissolved in vehicle and administered at 0.1 mL/30g mouse body weight for a dose of 3 mg/kg s.c. similar to as previously described (Dubocovich et al., 2005).

Data Analysis and Statistics.

All data analyses were done using GraphPad Prism 8™ software (Lo Jolla, CA). For *in vitro* binding studies, cpm were converted to percent total binding, with 100% defined as uninhibited 2-[^{125}I]-iodomelatonin binding and with 0% being nonspecific binding for each experiment. Concentration-response curves were fit to competition binding data using the equation “Y = Bottom + (Top - Bottom) / (1 + $10^{(X-LogEC_{50})}$)” (Slope = 1). Dissociation curves were fit to kinetic binding data using the equation “Y = (Y_0 -NS) * $e^{(-Koff*X)}$ + NS”. Top constraints were set to “100%” for all *in vitro* binding experiments. For structure-activity relationship and GTP shift competition binding studies, curve bottoms were constrained to “0%”. Bottoms of curves were constrained to be “greater

JPET Fast Forward. Published on November 17, 2020 as DOI: 10.1124/jpet.120.000065
This article has not been copyedited and formatted. The final version may differ from this version.

than 0" for binding titration and dissociation assays. For *in vitro* quantitative receptor autoradiography experiments curve bottoms were constrained to non-specific binding values determined for each set of adjacent sections analyzed. Individual K_i, K_B, and α values were calculated using commercial software (GraphPad Prism) according to the Cheng-Prusoff equation (Cheng and Prusoff, 1973; Lazareno and Birdsall, 1995). K_D values used in calculations correspond to specific receptors and conformation in buffer (hMT_1 active: 116 pM; hMT_1 resting: 280 pM; hMT_2 active: 119 pM; hMT_2 resting: 215 pM). 2-[^{125}I]-iodomelatonin dissociation rates (K_{off}) in the presence of test compounds are compared to vehicle using a Friedman test (alpha = 0.05) with Dunn's post-test for multiple comparisons (alpha = 0.05). Significant differences between $pK_{i(GTP)}$ and $pK_{i(Control)}$ were determined by two-tailed paired *t* tests (alpha = 0.05). Apparent efficacy at melatonin receptors of compounds was assessed by subtracting pK_i values obtained in active buffer from resting buffer ($pK_{i(GTP)}$-$pK_{i(Control)}$ = ΔpK_i) and comparison melatonin ΔpK_i (CHO-hMT_1: 1.19; CHO-hMT_2: 0.41). Affinity shifts or lack thereof between active and resting buffers indicate apparent efficacy (Lefkowitz et al., 1976; Nonno et al., 1998) thus ligands were characterized as agonists (ΔpK_i > 20 % MLT), antagonists (ΔpK_i < 20 % MLT, > -20 % MLT), or inverse agonists (ΔpK_i < -20 % MLT) accordingly. K_D used to determine IC_{50} for *in vitro* quantitative receptor autoradiography experiments was 87.3 pM (unpublished data). For *in vitro* and *ex vivo* quantitative receptor autoradiography data, average values for each treatment condition were compared to the control group (vehicle-treated) using one-way ANOVA (alpha = 0.05) with a Dunnet's post-test (alpha = 0.05) to assess differences between groups. For *in vivo* circadian rhythm experiments, circadian phase changes were compared via one-way ANOVA (alpha = 0.05) with a

JPET Fast Forward. Published on November 17, 2020 as DOI: 10.1124/jpet.120.000065
This article has not been copyedited and formatted. The final version may differ from this version.

Dunnet's post-test (alpha = 0.05) comparing carbaryl and melatonin to vehicle-treated mice.

JPET Fast Forward. Published on November 17, 2020 as DOI: 10.1124/jpet.120.000065
This article has not been copyedited and formatted. The final version may differ from this version.

8. RESULTS

Chemical Clustering of Environmental Toxins.

A search for a carbamate functional group in the Chem2Risk knowledgebase resulted in the identification of 8 carbamate insecticides (Figure 1A). In addition to carbaryl and carbofuran, which were previously identified as structurally similar to melatonin (Popovska-Gorevski et al., 2017), carbamate insecticides fenobucarb, fenoxycarb and bendiocarb cluster together with normalized Tanimoto structural similarity indices in 2D (S_{2D}) and 3D (S_{3D}) in the range 0.4 – 0.6 (Cluster 1; Figure 1B). Interestingly, all the carbamate insecticides in cluster 1 contain at least one aromatic ring system and a carbamate (–N-C(=O)-) moiety which aligns well with the melatonin pharmacophore. The carbamate insecticides aldicarb, methomyl and oxamyl, clustered together with very low structural similarly with S_{2D} and S_{3D} < 0.4 (cluster 2; Figure 1B).

Molecular Docking of Carbamate Insecticides to hMT_1 *and* hMT_2 *Receptors.*

Melatonin and the carbamate insecticides were docked into the putative melatonin binding pockets in hMT_1 and hMT_2 receptor models. Cluster 1-carbamate insecticides (carbaryl, carbofuran, bendiocarb, fenobucarb, and fenoxycarb) dock into the putative melatonin binding site with H195 (in hMT_1) or H208 (in hMT_2) within 2-3 *Å* similar to melatonin (Figure 2). Surflex docking experiments with cluster 1-carbamates yielded at least five docked poses per receptor-ligand complex where the ligand was positioned into the putative binding pocket were chosen for further analysis. Surflex docking scores of top ligand-hMT_2 receptor complexes were: melatonin (11.6; Figure 2G) > carbaryl (9.2; Figure 2H) > fenobucarb (8.9; Figure 2K) > bendiocarb (8.5; Figure

JPET Fast Forward. Published on November 17, 2020 as DOI: 10.1124/jpet.120.000065
This article has not been copyedited and formatted. The final version may differ from this version.

2l) > carbofuran (8.1; Figure 2L) > fenoxycarb (7.8; Figure 2J) whereas the corresponding scores for the ligand-hMT$_1$ complexes were: melatonin (11.9; Figure 2A) > fenobucarb (7.1; Figure 2E) > carbaryl (7.0; Figure 2B) > bendiocarb (5.6; Figure 2C) > carbofuran (5.1; Figure 2F) > fenoxycarb (4.7; Figure 2D). Root mean square deviation (RMSD) of the top 5 binding poses for each ligand-receptor complexes was < 2.0 Å. Autodock binding affinities of cluster 1-carbamate-MT$_2$ complexes were in the range -4 to -8 kcal/mol compared to -11.5 kcal/mol for melatonin-MT$_2$ complex consistent with the results of surflex docking scores. Based on these results, cluster 1-carbamates were predicted to mimic melatonin actions at MT$_1$ and MT$_2$ receptors and were propagated for further validation using receptor binding *in vitro*.

The recent availability of high-resolution x-ray crystal structures of melatonin receptors in complex with agomelatine, ramelteon, 2-iodomelatonin and 2-phenylmelatonin (Johansson et al., 2019; Stauch et al., 2019), post completion of the entire *in silico* to *in vivo* Chem2Risk pipeline, warranted a comparative analysis of the protein structures. A closer look at the ramelteon bound complexes reveals that it makes hydrogen binding contact with the amino acid residue Q181 and various non-binding contacts with A104, M107, G108, N162, L168, T178, F179, T188, V191 and L254 in the MT$_1$ melatonin receptor complex (PDB ID: 6ME2; MT$_1$-CC-ramelteon; (Stauch et al., 2019) and in MT$_2$ melatonin receptor complex it makes hydrogen binding contact with N175 and various non-bonding contacts with A117, M120, G121, V124, I125, L181, T191, F192, Q194, Y200, V204, V205, L267, N268 and G271 (PDB ID: 6ME9; MT$_2$-CC-ramelteon; (Johansson et al., 2019). Docking of top-scoring carbamate, carbaryl, into ramelteon binding pockets in hMT$_1$ and hMT$_2$ models derived from these

JPET Fast Forward. Published on November 17, 2020 as DOI: 10.1124/jpet.120.000065
This article has not been copyedited and formatted. The final version may differ from this version.

crystal structures show considerable overlap of binding pocket residues between the models used in our computational pipeline and the carbamate-melatonin receptor complexes generated using the x-ray crystal structures 6ME2-9. Top carbaryl-MT_1 docked poses indicate potential hydrogen bonding interactions at Q181 of hMT_1, like ramelteon (Supplemental Figure S1A), and at N175 or Q194 of hMT_2 (Supplemental Figure S1B). The residues N175 and H208 were within the 4 Å zone of the bound ligand carbaryl in MT_2 complexes consistent with our previously published model (Popovska-Gorevski et al., 2017).

Competition of Carbamate Insecticides for 2-[^{125}I]-Iodomelatonin Binding to hMT_1 *and* hMT_2 *Melatonin Receptors.*

Affinities for carbaryl, carbofuran, fenobucarb, fenoxycarb, bendiocarb, aldicarb, methomyl, and oxamyl (Figure 3) were determined by assessing competition for 2-[^{125}I]-iodomelatonin binding (75 pM) at hMT_1 and hMT_2 stably expressed in CHO cell membranes. All eight carbamates competed for 2-[^{125}I]-iodomelatonin binding at hMT_1 (K_i range = 3.34–1070 μM) and hMT_2 (K_i range = 0.163–438 μM; Figure 3; Table 1). Affinity constants (K_i values) for all compounds tested derived from competition with 2-[^{125}I]-iodomelatonin are listed in Table 1. Aldicarb, carbofuran, carbaryl, fenobucarb, bendiocarb, oxamyl, methomyl, and fenoxycarb displayed 55-, 26-, 20-, 18-, 14-, 2.6-, 2.4- and 1.1-fold selectivity for competition binding at hMT_2 compared to hMT_1 (Table 1) respectively. Rank order of affinities for competition binding of carbamate insecticides at hMT_1 is carbaryl > fenobucarb > fenoxycarb > bendiocarb > carbofuran > oxamyl >

JPET Fast Forward. Published on November 17, 2020 as DOI: 10.1124/jpet.120.000065
This article has not been copyedited and formatted. The final version may differ from this version.

aldicarb > methomyl and at hMT_2 is carbaryl > fenobucarb > bendiocarb > carbofuran > aldicarb > fenoxycarb > oxamyl > methomyl (Table 1).

Carbamate Insecticide Binding Mechanism(s) to hMT_1 *and* hMT_2 *Melatonin Receptors.* Next, we determined the mode of binding (i.e., orthosteric vs allosteric) of carbamate insecticides to the hMT_1 and hMT_2 melatonin receptors. Binding cooperativity factors (α) of melatonin, luzindole (a non-selective MT_1/MT_2 competitive receptor antagonist/inverse agonist) and carbaryl were derived from determining the maximal fractional inhibition (MFI) of 2-[^{125}I]-iodomelatonin binding at five different radioligand concentrations (30-1400 pM) to CHO-hMT_1 and CHO-hMT_2 membranes (Table S1). For both hMT_1 and hMT_2 receptors, melatonin (hMT_1 K_B = 0.220 nM, Figure S2A; hMT_2 K_B = 0.124 nM, Figure S2B) completely inhibited binding (hMT_1 and hMT_2 $\alpha < 0.001$, Figure S2A&B) of saturating concentrations of radioligand confirming both melatonin and 2-[^{125}I]-iodomelatonin bind to the same site. Luzindole (K_B = 13.8 nM, $\alpha < 0.001$, Figure S2D) and carbaryl (K_B = 453 nM, $\alpha < 0.001$, Figure 4B), also completely inhibited over 1000 pM 2-[^{125}I]-iodomelatonin binding at hMT_2 indicating that they bind to the orthosteric site. Interestingly, for luzindole (K_B = 387 nM, $\alpha = 0.037$, Figure S2C) and carbaryl (K_B = 3790 nM, $\alpha = 0.017$, Figure 4A) at hMT_1, the levels of maximal fractional inhibition of binding decreased with increasing concentrations of radioligand. Because 2-[^{125}I]-iodomelatonin is an agonist radioligand, additional titration tests for luzindole and carbaryl binding to CHO-hMT_1 membranes were conducted in resting buffer to minimize confounding effects associated with G protein coupling. Luzindole (K_B = 62.6 nM, $\alpha < 0.001$, Figure S2E) and carbaryl (K_B = 4400 nM, $\alpha < 0.001$, Figure 4C) completely

JPET Fast Forward. Published on November 17, 2020 as DOI: 10.1124/jpet.120.000065
This article has not been copyedited and formatted. The final version may differ from this version.

inhibited higher than 1000 pM 2-[^{125}I]-iodomelatonin binding at hMT_1 in resting buffer, thus providing supportive evidence of an orthosteric binding mechanism. To corroborate the likely orthosteric binding modes of the other cluster 1-carbamate insecticides, we tested their ability to alter the dissociation rate of 2-[^{125}I]-iodomelatonin from hMT_1 and hMT_2 bound in resting buffer. Alterations in radioligand dissociation rate by ligands, at concentrations lower than those that would significantly compete for binding with cold orthosteric dissociation initiators, are indicative of an allosteric binding mode. There were no rate differences detected in 2-[^{125}I]-iodomelatonin (100 pM) dissociation from hMT_1 and hMT_2 initiated by melatonin (10 μM) when tested in the absence (MT_1 VEH: 0.437 min^{-1}; MT_2 VEH: 0.0827 min^{-1}) or presence of test compounds (100 μM luzindole, carbaryl, fenobucarb, bendiocarb, or bendiocarb; Figure S3; Table S2).

Apparent Efficacy of Carbamate Insecticides as Determined in 2-[^{125}I]-Iodomelatonin GTP Shift Assays.

Affinity shifts for 2-[^{125}I]-iodomelatonin competition binding (75 pM) by carbamates with or without G protein inactivation by 100 μM GTP, 1 mM EDTA.Na_2 and 150 mM NaCl, were used to define apparent efficacy (affinity decrease/rightward shift for agonists, no change for antagonists, affinity increase/leftward shift for inverse agonists) (Lefkowitz et al., 1976; Nonno et al., 1998). For reference, in our system, competition binding in resting buffer decreased the affinity of full-agonist, melatonin, for both hMT_1 and hMT_2 receptors (hMT_1 $\Delta K_{i(GTP\text{-}control)}$ = -1.19; hMT_2 $\Delta K_{i(GTP\text{-}control)}$ = -0.41; Figures S4A,B, Table 3). Resting buffer did not change affinity for carbaryl, fenobucarb, bendiocarb or carbofuran at hMT_1 suggesting antagonist efficacy (Figures 5A, S4E,G;

JPET Fast Forward. Published on November 17, 2020 as DOI: 10.1124/jpet.120.000065
This article has not been copyedited and formatted. The final version may differ from this version.

Table 3; (Popovska-Gorevski et al., 2017) while at hMT_2, affinities are decreased displaying differences consistent with an agonist (Figures 5B, S4F,H; Table 3; (Popovska-Gorevski et al., 2017)).

In vitro Competition of Carbamate Insecticides for 2-[^{125}I]-Iodomelatonin Binding to Melatonin receptors in C3H/HeN Mouse Brain Slices (SCN, PVT, and PT).

Carbaryl, fenobucarb, and bendiocarb were selected for experiments in brain slices from mice based on their affinity at hMT_1 in CHO cells (Table 1). "Of note, quantitative receptor autoradiography in mouse brain tissue utilizing 2-[^{125}I]-iodomelatonin cannot detect quantifiable MT_2 receptor binding, as indicated by lack of specific radiolabeled sites in brain slices from MT_1 global knock out mice (Liu et al., 1997; Dubocovich et al., 1998). However, MT_2 melatonin receptor mRNA has been detected by in situ hybridization (Dubocovich et al., 1998; Hunt et al., 2001) and protein has been identified via immunohistochemistry in rodents (Lacoste et al., 2015). Further, attempts to label melatonin receptors with a MT_2 specific radioligand (Legros et al., 2016) failed to display specific binding in the SCN, PVNT, or PT further supporting that MT_2 levels in rodent brain are too low to detect via available melatonin receptor radioligands by quantitative receptor autoradiography. Representative autoradiograms of adjacent (20 µm) brain sections from a single WT mouse treated with vehicle, melatonin (1 µM), or carbaryl (1-100 µM) display a concentration-dependent decrease in visible 2-[^{125}I]-iodomelatonin labeling in the SCN, PVT, and PT (Figure 6). These images also reveal the expected competition by positive control melatonin (1 µM; non-specific binding; (Liu et al., 1997; Masana et al., 2000)-for 2-[^{125}I]-iodomelatonin binding

JPET Fast Forward. Published on November 17, 2020 as DOI: 10.1124/jpet.120.000065
This article has not been copyedited and formatted. The final version may differ from this version.

sites in the SCN, PVT, and PT (Figure 6A-B). Quantification of optical density in autoradiograms revealed that carbaryl competed in a concentration-dependent manner for 2-[^{125}I]-iodomelatonin (75 pM) binding in the SCN ($F_{3, 21}$ = 42.07, P < 0.001), in the PVT ($F_{3, 21}$ = 25.83, P < 0.0001) and the PT ($F_{3, 12}$ = 34.63, P < 0.0001) compared to vehicle-treated adjacent sections (Figure 7A-C; Supplemental Table 3). Similar competition was exhibited by carbaryl in brain slices from MT_2KO mice in the SCN ($F_{3,19}$ = 22.60, P < 0.001), PVT ($F_{3,16}$ = 22.19, P < 0.001), and PT ($F_{3,12}$ = 34.16, P < 0.001; Figure 7D-F; Supplemental Table 3). Fenobucarb and bendiocarb (1-100 μM) also competed in a concentration-dependent manner for 2-[^{125}I]-iodomelatonin (75 pM) binding in the SCN ($F_{3, 7}$ = 17.80, P < 0.001; $F_{3, 7}$ = 21.37, P < 0.001), in the PVT ($F_{3, 8}$ = 24.95, P < 0.001; $F_{3, 7}$ = 33.14, P < 0.001) and PT ($F_{4, 5}$ = 19.27, P < 0.01; $F_{4, 5}$ = 21.04, P < 0.01) compared to vehicle-treated adjacent sections (Supplemental Figure 5; Supplemental Table 4). Affinity (pK_i) values for carbaryl, fenobucarb and bendiocarb regarding competition for 2-[^{125}I]-iodomelatonin binding in these brain regions are shown in Table 2 and Supplemental Table 5. Across all treatments and experiments, mean non-specific binding determined by 1 μM melatonin was 31.65 ± 8.22%, 36.87± 8.82%, and 17.35 ± 5.82% in the SCN, PVT, and PT respectively.

Ex vivo Time Course for Competition of Carbaryl for 2-[^{125}I]-Iodomelatonin Binding in Brain Slices Containing the SCN.

Carbaryl was chosen for *in vivo* administration experiments due to its superior affinity at hMT_1 in recombinant receptors (Figure 3; Table 1) and potency at native mouse MT_1 (Figures 6 and 7; Table 2) compared to other carbamates tested. Of note,

JPET Fast Forward. Published on November 17, 2020 as DOI: 10.1124/jpet.120.000065
This article has not been copyedited and formatted. The final version may differ from this version.

ex vivo binding using 2[^{125}I]-iodomelatonin cannot detect quantifiable levels of specific binding to MT_2, allowing quantification of only MT_1 receptor affinity as previously mentioned. *In vivo* administration of carbaryl (10 mg/kg, i.p.) reduced specific 2-[^{125}I]-iodomelatonin binding (50 pM) in SCN brain slices processed *ex vivo* at 30, 60, and 120 minutes post-administration compared to vehicle-treated mice ($F_{4,23}$ = 13.21, P < 0.001), which recovered by 240 minutes (Figure 8A; Supplemental Table 3). Carbaryl also reduced specific 2-[^{125}I]-iodomelatonin binding (50 pM) in PVT brain slices processed *ex vivo* ($F_{4,23}$ = 5.79, P < 0.01; Figure 8B; Supplemental Table 3). Interestingly, specific binding in the PVT was found to be specifically increased at 240 minutes vs control sections (Figure 8B; Supplemental Table 3). In the PT, specific 2-[^{125}I]-iodomelatonin binding was reduced by carbaryl only at 60 minutes post-administration (P < 0.05; Figure 8C).

In vivo Administration of Carbaryl at CT 10 Phase-Advances Onset of Circadian Running Wheel Activity Rhythms.

Figure 9 (A, B, C) shows representative actograms for single mice treated with vehicle (15% ethanol/saline), melatonin (3 mg/kg, s.c.) or carbaryl (10 mg/kg, i.p.) for 3 consecutive days at CT 10, two hours before onset of activity (CT12). Quantification of phase shifts indicates that positive control melatonin and experimental drug carbaryl produce significant phase advances of onset of activity rhythms compared to vehicle-treated controls ($F_{2,20}$=18.46; P < 0.05; Dunnet's Post Test; Figure 9D; Supplemental Table 3). A single mouse was excluded from the carbaryl treatment group due to

JPET Fast Forward. Published on November 17, 2020 as DOI: 10.1124/jpet.120.000065
This article has not been copyedited and formatted. The final version may differ from this version.

meeting exclusion criterion of 2/3 injections falling outside of the acceptable range (CT 9 - 11).

JPET Fast Forward. Published on November 17, 2020 as DOI: 10.1124/jpet.120.000065
This article has not been copyedited and formatted. The final version may differ from this version.

9. DISCUSSION

Carbamate insecticides sharing high structural similarity to melatonin, bind competitively to the orthosteric site of the human recombinant MT_1 and MT_2 melatonin receptors. Pharmacological data validated *in silico* and pharmacoinformatic predictions for carbamates demonstrating binding to the orthosteric sites of melatonin receptors with antagonist apparent efficacy for hMT_1 and agonist apparent efficacy for hMT_2 receptors. Further, carbaryl competed for 2-[^{125}I]-iodomelatonin binding in mouse brain areas with high expression of melatonin receptors involved in the modulation of circadian (i.e., SCN), neurochemical as well as behavioral (i.e., PVT), and endocrine (i.e., PT) functions. Lastly, carbaryl phase-shifted overt circadian activity rhythm onsets akin to melatonin when given to C3H/HeN wild type mice two hours before (CT 10) onset of activity (CT 12). Here we discuss implications for these novel properties of carbamate insecticides in toxicological outcomes not explained by canonical actions at AChE as well as potential limitations of the present data.

The Chem2risk knowledge-based pipeline was used to discover environmental melatonin receptor ligands. Cluster 1-carbamate insecticides (carbaryl, carbofuran, fenobucarb, bendiocarb, and fenoxycarb), with Tanimoto indices S_{2D} and S_{3D} > 0.4, possess typical melatonin pharmacophore fingerprints which include an aromatic ring system and a carbonyl moiety in position to leverage interactions with the binding site residues H195 or Q181 in MT_1 and N175, Q194 or H208 in MT_2. Comparative molecular docking of top carbamates with the recently reported crystal structures (Johansson et al., 2019; Stauch et al., 2019) revealed a considerable overlap of binding pocket residues. Carbamate insecticides competitively bind to the MT_1 and MT_2 melatonin

JPET Fast Forward. Published on November 17, 2020 as DOI: 10.1124/jpet.120.000065
This article has not been copyedited and formatted. The final version may differ from this version.

receptor orthosteric sites likely formed by the aforementioned residues (Lazareno and Birdsall, 1995; Kenakin, 2009). The higher selectivity of carbaryl for binding to the hMT_2 receptors over the hMT_1 (33-fold) (Popovska-Gorevski et al., 2017) is likely attributed to the ring stacking interactions with H208 and partial occupancy of the hydrophobic cavity formed by the residues V124, I125, P212, I213, and F260 similar to reported ligand binding modes of selective MT_2 ligands (Rivara et al., 2005; Pala et al., 2013a; Pala et al., 2013b; Jockers et al., 2016; Johansson et al., 2019). Carbamates, carbaryl, bendiocarb, and fenobucarb competed for mMT_1 receptors expressed in the SCN, PVT, and PT in C3H/HeN mouse brain slices yielding pK_i values similar to the affinity constants for binding at recombinant hMT_1 receptors expressed in CHO cells. Altogether, our computational predictions were translatable interactions for recombinant human and endogenous mouse melatonin receptors and suggest these model systems may be useful in risk assessment of environmental compounds to human health based on success here with predictions relevant to the melatonin system.

Ex vivo quantitative receptor autoradiography data from the current report are in line with previously reported findings for the temporal pharmacokinetic (Declume and Benard, 1977; Krolski et al., 2003), biochemical (Moser et al., 2012; Wang et al., 2014; Moser et al., 2015a; Moser et al., 2015b), and behavioral effects of carbaryl (Albright and Simmel, 1979; Ruppert et al., 1983b; Moser et al., 1988; Moser, 1995). Peak effects on behavior, brain cholinesterase inhibition, and radiolabeled drug recovery in brain tissue occur from 30 –120 minutes post-delivery of carbaryl depending on the route of administration. Therefore, our results from time course experiments showing *ex vivo* competition binding of carbaryl at mouse melatonin receptors maximally at 60

JPET Fast Forward. Published on November 17, 2020 as DOI: 10.1124/jpet.120.000065
This article has not been copyedited and formatted. The final version may differ from this version.

minutes post-administration in brain areas expressing mMT_1 melatonin receptors (SCN, PT) are in agreement with reported temporal presentation of effects on behavior and bio-distribution to the brain related to interactions with cholinergic systems. This study was admittedly limited in that we did not explore exact brain concentrations of carbaryl when administered at 10 mg/kg i.p., however this carbamate dose clearly shows binding to melatonin receptors in the SCN and phase advances circadian phase. Maximal functional response for phase shift at CT 10 are obtained with 1 and 3 mg/kg melatonin acting on brain MT_1 melatonin receptors in the SCN (Benloucif and Dubocovich, 1996; Dubocovich et al., 1998; Stein et al., 2020). In the present study carbaryl also competed *ex vivo* for 2-[^{125}I]-iodomelatonin binding sites (SCN, PVT, PT) in mouse brain slices after *in vivo* administration and induced a maximal phase advance (compared to melatonin) of the onset of circadian activity rhythms in a translational behavioral mouse model. The present data demonstrate interactions of carbaryl and/or metabolites, and/or melatonin itself as carbaryl can increase its production (Attia et al., 1991a; Attia et al., 1991b) at brain melatonin receptors with resulting behavioral effects on circadian rhythms.

Acute carbaryl administration 2 hours before onset of activity (CT 10) phase-shifts circadian activity rhythms similarly to melatonin receptor agonists (Dubocovich et al., 2005; Liu et al., 2016) in contrast to present results from GTP-shift assays suggesting antagonist apparent efficacy. Behavioral efficacy of compounds acting at melatonin receptors has been shown to vary with time of administration as well as chronobiological context (Stein et al., 2020), suggesting the need to test carbaryl at other times in the circadian cycle sensitive to melatonin receptor stimulation (i.e., CT 1 -

JPET Fast Forward. Published on November 17, 2020 as DOI: 10.1124/jpet.120.000065
This article has not been copyedited and formatted. The final version may differ from this version.

3) (Benloucif and Dubocovich, 1996) or in the jet-lag paradigm (Dubocovich et al., 2005). Drug-mediated phase shifts directly translate from the C3H/HeN mouse to human models (Benloucif and Dubocovich, 1996; Burgess et al., 2008). Therefore, carbaryl could be a possible circadian modulator in humans via actions at SCN melatonin receptors. However, it's possible carbaryl exposure may also influence circadian physiology through reported modulation of pineal and blood melatonin levels, levels of pineal serotonin as well as it's precursors, and hypothalamic uptake of norepinephrine (Jablonska and Brzezinski, 1990; Attia et al., 1991a; Attia et al., 1991b). Therefore, carbaryl may dually regulate the synthesis of melatonin and also directly compete for binding at melatonin receptors to influence mediated processes. Context for melatonin receptor signaling and physiological relevance are also important considerations as time-of-day (Benloucif and Dubocovich, 1996; Gillette and Mitchell, 2002) and protein composition of the system under study (Liu et al., 2019) can significantly impact results interpretation. Lastly, we must also acknowledge the ability of the cholinergic system to influence phase of circadian rhythms on its own (Liu and Gillette, 1996). However, the peak of sensitivity for cholinergic regulation of circadian rhythms (CT 17 - 19) is outside the sensitive periods (CT 1 - 3 and 9 - 11) for modulation of circadian rhythms by melatonin receptor agonists (Benloucif and Dubocovich, 1996; Dubocovich et al., 2005).

Several other off-target receptors and proteins could contribute to the phase resetting effect of carbaryl. The PubChem BioAssay Database (https://pubchem.ncbi.nlm.nih.gov), with over 1700 entries from biological screening platforms such as ChEMBL (https://www.ebi.ac.uk/chembl/), Tox21

JPET Fast Forward. Published on November 17, 2020 as DOI: 10.1124/jpet.120.000065
This article has not been copyedited and formatted. The final version may differ from this version.

(https://ntp.niehs.nih.gov/whatwestudy/tox21/toolbox/index.html), and NCATS (https://ncats.nih.gov/etb), lists potential carbaryl targets at concentrations below 10 μM to include the pregnane X receptor (potency = 3.2 μM; Tox21) and the aryl hydrocarbon receptor (AhR; potency = 5.3 μM; Tox21). Environmental dioxins alter circadian rhythms via AhR mediated-interference of clock gene transcription and phase resetting-induced by light pulses in mice (Xu et al., 2010; Tischkau et al., 2011; Xu et al., 2013). Dioxins affect clock genes and behavioral rhythms contributing to altered glucose metabolism, insulin resistance, and sleep disorders. However, the time of circadian sensitivity for these effects has not been reported, thus making comparisons with the range of sensitivity for melatonin receptor-mediated phase shifts of circadian activity difficult. Action of carbaryl at other proteins was also investigated using the National Institute of Mental Health Psychoactive Drug Screening Program (NIHM PDSP) screening for inhibition of radioligand binding at 40 GPCR targets, which only revealed affinity for $5HT_{2B}$ receptors (Besnard et al., 2012). Carbaryl affinity for $5HT_{2B}$ (K_i = 5.2 μM) suggests that we cannot rule out action actions at this receptor, however, serotonin maximally modulates circadian phase at ZT 6 (Prosser et al., 1993; Gillette and Mitchell, 2002) and there is no evidence that $5HT_{2B}$ activity modulates circadian biology.

Routes of exposure for carbaryl in the general population range from inhalation and dermal exposure predominately at occupational sites, to oral exposure from contaminated food and water supplies on the environmental side (HSDB NLM, Gunaskara, Rubin et al. 2008). The level of daily exposure to carbamate insecticides in humans not occupationally exposed is reportedly 0.02 - 0.12 μg/kg body weight/day or 1.4 - 8.4 μg/day from dietary sources (Duggan et al., 1983; Gartrell et al., 1985; Gartrell

JPET Fast Forward. Published on November 17, 2020 as DOI: 10.1124/jpet.120.000065
This article has not been copyedited and formatted. The final version may differ from this version.

et al., 1986); HSDB NLM). Carbaryl does not accumulate in the body as it is rapidly metabolized to 1-naphthol which is used as a biomarker of exposure (Shealy et al., 1997; Gunaskara et al., 2008). Doses of carbaryl required to produce cholinergic effects are generally higher than the dose used in the present study (10 mg/kg, i.p.) to compete for binding at brain melatonin receptors *ex vivo* as well as to phase-shift circadian activity rhythms in C3H/HeN mice. Doses of carbaryl that produce clinically significant cholinesterase inhibition in brain and blood are equal to or above 15 mg/kg i.p. or oral gavage (Ruppert et al., 1983a), with one study finding no effects of carbaryl on brain cholinesterase activity with doses up to 42.5 mg/kg via oral gavage (Wang et al., 2014). Conversely, another study by Moser et al. (2015a) found that doses of 3 & 7.5 mg/kg carbaryl via oral gavage significantly reduced brain and blood cholinesterase activity by 10 - 30% and 30 - 50% respectively compared to controls. However, many of the behavioral and physiological effects of carbaryl attributable to effects on the cholinergic system (altered gait, reduced motor responses, convulsions, ptosis, lacrimation, salivation, chewing, decreased body temperature, etc.) are not exhibited in rodent studies until doses of at least 20 - 30 mg/kg given i.p. or via oral gavage, with effects only on decreased pupil response and increased ptosis seen below this range at 10 mg/kg i.p. (Moser et al., 1988). Thus, it seems possible that the toxicological implications of carbaryl could be more relevant to the melatonin vs. the cholinergic system based on doses required for physiological and clinically relevant effects. Future studies will determine dose relevance below 10 mg/kg i.p. to address external validity issues with matching environmentally relevant exposure doses for effects of carbaryl on phase shift of circadian rhythms and other chronobiological behaviors.

JPET Fast Forward. Published on November 17, 2020 as DOI: 10.1124/jpet.120.000065
This article has not been copyedited and formatted. The final version may differ from this version.

Our data highlight novel pharmacological properties of carbamate insecticides at melatonin receptors. Carbamates like carbaryl display unique pharmacological properties suggesting their potential to alter physiologically relevant responses independent of or in addition to canonical actions at AChE activity. Based on our data we suggest that pharmacological actions of carbamate insecticides at melatonin receptors should be investigated for potential to produce: a) mistimed melatonin receptor activation, b) alterations of melatonin rhythms by activating and/or blocking timing cues at nonoptimal times of day, or by mistimed phase shifts leading to circadian rhythm desynchronization, c) disrupted timing of physiological processes under control of melatonin-mediated time-of-day signaling (i.e., modulation of pancreas metabolic rhythmicity), and/or d) modulation of core clock gene transcription or rhythmicity. These changes could predispose or contribute to relevant disease pathologies observed after exposure to carbamate insecticides linked indirectly to circadian disruption, particularly those not explained by actions at AChE, such as sleep apnea (Zirlik et al., 2013; Baumert et al., 2018).

JPET Fast Forward. Published on November 17, 2020 as DOI: 10.1124/jpet.120.000065
This article has not been copyedited and formatted. The final version may differ from this version.

10. ACKNOWLEDGMENTS

We would like to thank Dr. Shannon Clough for expert suggestions and technical advice in experiments involving mice and Dr. Gregory Wilding from the UB Clinical and Translational Science Institute Biostatistics, Epidemiology and Research Design (BERD) Core for advice on statistical analyses of *in vivo* experimental data.

The receptor binding profile of carbaryl was generously provided by the National Institute of Mental Health's Psychoactive Drug Screening Program, Contract # HHSN-271-2018-00023-C (NIMH PDSP). The NIMH PDSP is directed by Bryan L. Roth M.D., Ph.D. at the University of North Carolina at Chapel Hill and Project Officer Jamie Driscoll at NIMH, Bethesda MD, USA.

11. AUTHOR CONTRIBUTIONS

Research design: A.J.J., G.C.G., R.V.R., M.L.D.

In silico experiments and analyses: R.V.R.

In vitro experiments and analyses: A.J.J, G.C.G

In vivo experiments and analyses: G.C.G.

Wrote and contributed to the writing of the manuscript: A.J.J., G.C.G., R.V.R., M.L.D.

12. REFERENCES

Albright ME and Simmel EC (1979) Behavioral effects of the cholinesterase inhibitor and insecticide carbaryl (Sevin). *Journal of Biological Psychology* **21**:25-31.

Ali SA, Khan SA, Naaz I and Ali AS (2015) Adverse health effects of pesticide exposure in workers of a pesticide manufacturing factory. *Bioscience Biotechnology Research Communications* **8**:208-212.

Attia AM, Reiter RJ, Nonaka KO, Mostafa MH, Soliman SA and el-Sebae AH (1991a) Carbaryl-induced changes in indoleamine synthesis in the pineal gland and its effects on nighttime serum melatonin concentrations. *Toxicology* **65**:305-314.

Attia AM, Reiter RJ, Withyachumnarnkul B, Mostafa MH, Soliman SA and el-sebae AK (1991b) Chronic administration of sublethal doses of carbaryl increases pineal N-acetyltransferase and hydroxyindole-O-methyltransferase activities and serum melatonin levels. *J Pineal Res* **10**:49-54.

Baron KG and Reid KJ (2014) Circadian misalignment and health. *Int Rev Psychiatry* **26**:139-154.

Baumert BO, Carnes MU, Hoppin JA, Jackson CL, Sandler DP, Freeman LB, Henneberger PK, Umbach DM, Shrestha S, Long S and London SJ (2018) Sleep apnea and pesticide exposure in a study of US farmers. *Sleep Health* **4**:20-26.

Benloucif S and Dubocovich ML (1996) Melatonin and light induce phase shifts of circadian activity rhythms in the C3H/HeN mouse. *J Biol Rhythms* **11**:113-125.

Benloucif S, Masana MI and Dubocovich ML (1997) Responsiveness to melatonin and its receptor expression in the aging circadian clock of mice. *Am J Physiol* **273**:R1855-1860.

Benloucif S, Masana MI, Yun K and Dubocovich ML (1999) Interactions between light and melatonin on the circadian clock of mice. *J Biol Rhythms* **14**:281-289.

Beresford IJM, Browning C, Starkey SJ, Brown J, Foord SM, Coughlan J, North PC, Dubocovich ML and Hagan RM (1998) GR196429: A nonindolic agonist at high-affinity melatonin receptors. *Journal of Pharmacology and Experimental Therapeutics* **285**:1239-1245.

Besnard J, Ruda GF, Setola V, Abecassis K, Rodriguiz RM, Huang XP, Norval S, Sassano MF, Shin AI, Webster LA, Simeons FR, Stojanovski L, Prat A, Seidah NG, Constam DB, Bickerton GR, Read KD, Wetsel WC, Gilbert IH, Roth BL and Hopkins AL (2012) Automated design of ligands to polypharmacological profiles. *Nature* **492**:215-220.

Bini Dhouib I, Annabi A, Jallouli M, Marzouki S, Gharbi N, Elfazaa S and Lasram MM (2016) Carbamates pesticides induced immunotoxicity and carcinogenicity in human: A review. *Journal of Applied Biomedicine*.

Bothorel B, Barassin S, Saboureau M, Perreau S, Vivien-Roels B, Malan A and Pevet P (2002) In the rat, exogenous melatonin increases the amplitude of pineal melatonin secretion by a direct action on the circadian clock. *Eur J Neurosci* **16**:1090-1098.

Burgess HJ, Revell VL and Eastman CI (2008) A three pulse phase response curve to three milligrams of melatonin in humans. *J Physiol* **586**:639-647.

Casida JE (1963) Mode of action of carbamates. *Annual review of entomology* **8**:39-58.

Casida JE and Bryant RJ (2017) The ABCs of pesticide toxicology: amounts, biology, and chemistry. *Toxicol Res (Camb)* **6**:755-763.

Cheng Y and Prusoff WH (1973) Relationship between the inhibition constant (K1) and the concentration of inhibitor which causes 50 per cent inhibition (I50) of an enzymatic reaction. *Biochemical pharmacology* **22**:3099-3108.

Clark-Reyna SE, Grineski SE and Collins TW (2016) Ambient Concentrations of Metabolic Disrupting Chemicals and Children's Academic Achievement in El Paso, Texas. *Int J Environ Res Public Health* **13**.

Declume C and Benard P (1977) FOETAL ACCUMULATION OF ['4C] CARBARYL IN RATS AND MICE AUTORADIOGRAPHIC STUDY. *Toxicology* **8**:95-105.

Dubocovich ML (2007) Melatonin receptors: role on sleep and circadian rhythm regulation. *Sleep medicine* **8 Suppl 3**:34-42.

Dubocovich ML, Delagrange P, Krause DN, Sugden D, Cardinali DP and Olcese J (2010) International Union of Basic and Clinical Pharmacology. LXXV. Nomenclature, classification, and pharmacology of G protein-coupled melatonin receptors. *Pharmacological reviews* **62**:343-380.

Dubocovich ML, Hudson RL, Sumaya IC, Masana MI and Manna E (2005) Effect of MT1 melatonin receptor deletion on melatonin-mediated phase shift of circadian rhythms in the C57BL/6 mouse. *J Pineal Res* **39**:113-120.

Dubocovich ML and Markowska M (2005) Functional MT1 and MT2 melatonin receptors in mammals. *Endocrine* **27**:101-110.

Dubocovich ML, Yun K, Al-Ghoul WM, Benloucif S and Masana MI (1998) Selective MT2 melatonin receptor antagonists block melatonin-mediated phase advances of circadian rhythms. *Faseb j* **12**:1211-1220.

Duggan RE, Corneliussen PE, Duggan MB, McMahon BM and Martin RJ (1983) Pesticide residue levels in foods in the United States from July 1, 1969, to June 30, 1976: Summary. *Journal - Association of Official Analytical Chemists* **66**:1534-1535.

Ecobichon DJ (2001) Pesticide use in developing countries. *Toxicology* **160**:27-33.

Gartrell MJ, Craun JC, Podrebarac DS and Gunderson EL (1985) Pesticides, selected elements, and other chemicals in adult total diet samples, October 1979-September 1980. *Journal - Association of Official Analytical Chemists* **68**:1184-1197.

Gartrell MJ, Craun JC, Podrebarac DS and Gunderson EL (1986) Pesticides, selected elements, and other chemicals in adult total diet samples, October 1980-March 1982. *Journal - Association of Official Analytical Chemists* **69**:146-159.

Gerdin MJ, Masana MI, Ren D, Miller RJ and Dubocovich ML (2003) Short-term exposure to melatonin differentially affects the functional sensitivity and trafficking of the hMT1 and hMT2 melatonin receptors. *The Journal of pharmacology and experimental therapeutics* **304**:931-939.

Gillette MU and Mitchell JW (2002) Signaling in the suprachiasmatic nucleus: selectively responsive and integrative. *Cell Tissue Res* **309**:99-107.

Gunaskara AS, Rubin AL, Goh KS, Spurlock FC and Tjeerdema RS (2008) Environmental fate and toxicology of carbaryl. *Reviews of Environmetnal Contamination and Toxicology* **196**:95.

Hunt AE, Al-Ghoul WM, Gillette MU and Dubocovich ML (2001) Activation of MT(2) melatonin receptors in rat suprachiasmatic nucleus phase advances the circadian clock. *Am J Physiol Cell Physiol* **280**:C110-118.

Hutchinson AJ, Hudson RL and Dubocovich ML (2012) Genetic deletion of MT(1) and MT(2) melatonin receptors differentially abrogates the development and expression of methamphetamine-induced locomotor sensitization during the day and the night in C3H/HeN mice. *J Pineal Res* **53**:399-409.

Jablonska J and Brzezinski J (1990) The influence of carbaryl on the uptake of (3H)-noradrenaline (3H)-NA by rat hypothalamic slices. *Arch Toxicol* **64**:417-419.

Jockers R, Delagrange P, Dubocovich ML, Markus RP, Renault N, Tosini G, Cecon E and Zlotos DP (2016) Update on melatonin receptors: IUPHAR Review 20. *British journal of pharmacology* **173**:2702-2725.

Johansson LC, Stauch B, McCorvy JD, Han GW, Patel N, Huang XP, Batyuk A, Gati C, Slocum ST, Li C, Grandner JM, Hao S, Olsen RHJ, Tribo AR, Zaare S, Zhu L, Zatsepin NA, Weierstall U, Yous S, Stevens RC, Liu W, Roth BL, Katritch V and Cherezov V (2019) XFEL structures of the human MT2 melatonin receptor reveal the basis of subtype selectivity. *Nature* **569**:289-292.

Karamitri A and Jockers R (2019) Melatonin in type 2 diabetes mellitus and obesity. *Nat Rev Endocrinol* **15**:105-125.

Kavlock RJ, Austin CP and Tice RR (2009) Toxicity testing in the 21st century: implications for human health risk assessment. *Risk analysis : an official publication of the Society for Risk Analysis* **29**:485-487; discussion 492-487.

Kenakin TP (2009) Chapter 4 - Pharmacological Assay Formats: Binding, in *A Pharmacology Primer (Third Edition)* (Kenakin TP ed) pp 61-79, Academic Press, New York.

Krolski ME, Nguyen T, Lopez R, YIng L-L and Roensch W (2003) Metabolism and pharmacokinetics of [14C]-carbaryl in rats following mixed oral and dermal exposure. *Bayer CropScience* **169-0746**.

Lacoste B, Angeloni D, Dominguez-Lopez S, Calderoni S, Mauro A, Fraschini F, Descarries L and Gobbi G (2015) Anatomical and cellular localization of melatonin MT1 and MT2 receptors in the adult rat brain. *J Pineal Res* **58**:397-417.

Lazareno S and Birdsall NJ (1995) Detection, quantitation, and verification of allosteric interactions of agents with labeled and unlabeled ligands at G protein-coupled receptors: interactions of strychnine and acetylcholine at muscarinic receptors. *Mol Pharmacol* **48**:362-378.

Lebov JF, Engel LS, Richardson D, Hogan SL, Sandler DP and Hoppin JA (2015) Pesticide exposure and end-stage renal disease risk among wives of pesticide applicators in the Agricultural Health Study. *Environ Res* **143**:198-210.

Lefkowitz RJ, Mullikin D and Caron MG (1976) Regulation of beta-adrenergic receptors by guanyl-5'-yl imidodiphosphate and other purine nucleotides. *The Journal of biological chemistry* **251**:4686-4692.

Legros C, Brasseur C, Delagrange P, Ducrot P, Nosjean O and Boutin JA (2016) Alternative Radioligands for Investigating the Molecular Pharmacology of

Melatonin Receptors. *Journal of Pharmacology and Experimental Therapeutics* **356**:681-692.

Liu C and Gillette MU (1996) Cholinergic regulation of the suprachiasmatic nucleus circadian rhythm via a muscarinic mechanism at night. *The Journal of neuroscience : the official journal of the Society for Neuroscience* **16**:744-751.

Liu C, Weaver DR, Jin X, Shearman LP, Pieschl RL, Gribkoff VK and Reppert SM (1997) Molecular dissection of two distinct actions of melatonin on the suprachiasmatic circadian clock. *Neuron* **19**:91-102.

Liu J, Clough SJ, Hutchinson AJ, Adamah-Biassi EB, Popovska-Gorevski M and Dubocovich ML (2016) MT1 and MT2 Melatonin Receptors: A Therapeutic Perspective. *Annual review of pharmacology and toxicology* **56**:361-383.

Liu L, Labani N, Cecon E and Jockers R (2019) Melatonin Target Proteins: Too Many or Not Enough? *Front Endocrinol (Lausanne)* **10**:791.

Mahajan R, Blair A, Coble J, Lynch CF, Hoppin JA, Sandler DP and Alavanja MC (2007) Carbaryl exposure and incident cancer in the Agricultural Health Study. *International journal of cancer* **121**:1799-1805.

Manyilizu WB and Mdegela RH (2015) Self-reported Health Effects among Short and Long-term Pesticide Sprayers in Arusha, Northern Tanzania: A cross Sectional Study. *Occupational Medicine & Health Affairs* **03**.

Masana MI, Benloucif S and Dubocovich ML (2000) Circadian rhythm of mt1 melatonin receptor expression in the suprachiasmatic nucleus of the C3H/HeN mouse. *J Pineal Res* **28**:185-192.

Meeker JD, Ryan L, Barr DB, Herrick RF, Bennett DH, Bravo R and Hauser R (2004) The relationship of urinary metabolites of carbaryl/naphthalene and chlorpyrifos with human semen quality. *Environmental health perspectives* **112**:1665-1670.

Meyer A, Sandler DP, Beane Freeman LE, Hofmann JN and Parks CG (2017) Pesticide Exposure and Risk of Rheumatoid Arthritis among Licensed Male Pesticide Applicators in the Agricultural Health Study. *Environmental health perspectives* **125**:077010.

Miller JA and Zahniser NR (1987) The use of 14C-labeled tissue paste standards for the calibration of 125I-labeled ligands in quantitative autoradiography. *Neurosci Lett* **81**:345-350.

Montgomery MP, Kamel F, Saldana TM, Alavanja MC and Sandler DP (2008) Incident diabetes and pesticide exposure among licensed pesticide applicators: Agricultural Health Study, 1993-2003. *Am J Epidemiol* **167**:1235-1246.

Moser VC (1995) Comparison of the acute effects of cholinesterase inhibitors using a neurobehavioral screening battery in rats. *Neurotoxicology and teratology* **17**:617-625.

Moser VC, McCormick JP, Creason JP and MacPhail RC (1988) Comparison of chlordimeform and carbaryl using a functional observational battery. *Fundamental and Applied Toxicology* **11**:189-206.

Moser VC, Padilla S, Simmons JE, Haber LT and Hertzberg RC (2012) Impact of chemical proportions on the acute neurotoxicity of a mixture of seven carbamates in preweanling and adult rats. *Toxicological sciences : an official journal of the Society of Toxicology* **129**:126-134.

Moser VC, Phillips PM and McDaniel KL (2015a) Assessment of biochemical and behavioral effects of carbaryl and methomyl in Brown-Norway rats from preweaning to senescence. *Toxicology* **331**:1-13.

Moser VC, Stewart N, Freeborn DL, Crooks J, MacMillan DK, Hedge JM, Wood CE, McMahen RL, Strynar MJ and Herr DW (2015b) Assessment of serum biomarkers in rats after exposure to pesticides of different chemical classes. *Toxicology and applied pharmacology* **282**:161-174.

Nonno R, Lucini V, Pannacci M, Mazzucchelli C, Angeloni D, Fraschini F and Stankov BM (1998) Pharmacological characterization of the human melatonin Mel1a receptor following stable transfection into NIH3T3 cells. *British journal of pharmacology* **124**:485-492.

Pala D, Beuming T, Sherman W, Lodola A, Rivara S and Mor M (2013a) Structure-based virtual screening of MT2 melatonin receptor: influence of template choice and structural refinement. *J Chem Inf Model* **53**:821-835.

Pala D, Lodola A, Bedini A, Spadoni G and Rivara S (2013b) Homology models of melatonin receptors: challenges and recent advances. *Int J Mol Sci* **14**:8093-8121.

Patel O, Syamlal G, Henneberger PK, Alarcon WA and Mazurek JM (2018) Pesticide use, allergic rhinitis, and asthma among US farm operators. *Journal of agromedicine* **23**:327-335.

Patel S and Sangeeta S (2019) Pesticides as the drivers of neuropsychotic diseases, cancers, and teratogenicity among agro-workers as well as general public. *Environ Sci Pollut Res Int* **26**:91-100.

Peschke E, Bahr I and Muhlbauer E (2013) Melatonin and pancreatic islets: interrelationships between melatonin, insulin and glucagon. *Int J Mol Sci* **14**:6981-7015.

Popovska-Gorevski M, Dubocovich ML and Rajnarayanan RV (2017) Carbamate Insecticides Target Human Melatonin Receptors. *Chem Res Toxicol* **30**:574-582.

Prosser RA, Dean RR, Edgar DM, Heller HC and Miller JD (1993) Serotonin and the mammalian circadian system: I. In vitro phase shifts by serotonergic agonists and antagonists. *J Biol Rhythms* **8**:1-16.

Rivara S, Lorenzi S, Mor M, Plazzi PV, Spadoni G, Bedini A and Tarzia G (2005) Analysis of structure-activity relationships for MT2 selective antagonists by melatonin MT1 and MT2 receptor models. *J Med Chem* **48**:4049-4060.

Ruppert PH, Cook LL, Dean KF and Reiter LW (1983a) Acute behavioral toxicity of carbaryl and propoxur in adult rats. *Pharmacol Biochem Behav* **18**:579-584.

Ruppert PH, Cook LL, Dean KF and Reiter LW (1983b) Acute behavioral toxicity of carbaryl and propoxur in adult rats. *Pharm Biochem Behav* **18**:579-584.

Saldana TM, Basso O, Hoppin JA, Baird DD, Knott C, Blair A, Alavanja MC and Sandler DP (2007) Pesticide exposure and self-reported gestational diabetes mellitus in the Agricultural Health Study. *Diabetes Care* **30**:529-534.

Schmidt CW (2009) TOX 21: new dimensions of toxicity testing. *Environmental health perspectives* **117**:A348-353.

Schroeder AM and Colwell CS (2013) How to fix a broken clock. *Trends Pharmacol Sci* **34**:605-619.

Shealy DB, Barr JR, Ashley DL, Patterson DG, Jr., Camann DE and Bond AE (1997) Correlation of environmental carbaryl measurements with serum and urinary 1-naphthol measurements in a farmer applicator and his family. *Environmental health perspectives* **105**:510-513.

Siuciak JA, Fang JM and Dubocovich ML (1990) Autoradiographic localization of 2-[125I]iodomelatonin binding sites in the brains of C3H/HeN and C57BL/6J strains of mice. *Eur J Pharmacol* **180**:387-390.

Slager RE, Simpson SL, Levan TD, Poole JA, Sandler DP and Hoppin JA (2010) Rhinitis associated with pesticide use among private pesticide applicators in the agricultural health study. *J Toxicol Environ Health A* **73**:1382-1393.

Stauch B, Johansson LC and Cherezov V (2020) Structural insights into melatonin receptors. *The FEBS Journal* **287**:1496-1510.

Stauch B, Johansson LC, McCorvy JD, Patel N, Han GW, Huang XP, Gati C, Batyuk A, Slocum ST, Ishchenko A, Brehm W, White TA, Michaelian N, Madsen C, Zhu L, Grant TD, Grandner JM, Shiriaeva A, Olsen RHJ, Tribo AR, Yous S, Stevens RC, Weierstall U, Katritch V, Roth BL, Liu W and Cherezov V (2019) Structural basis of ligand recognition at the human MT1 melatonin receptor. *Nature* **569**:284-288.

Stein RM, Kang HJ, McCorvy JD, Glatfelter GC, Jones AJ, Che T, Slocum S, Huang XP, Savych O, Moroz YS, Stauch B, Johansson LC, Cherezov V, Kenakin T, Irwin JJ, Shoichet BK, Roth BL and Dubocovich ML (2020) Virtual discovery of melatonin receptor ligands to modulate circadian rhythms. *Nature* **579**:609-614.

Sulkava S, Muggalla P, Sulkava R, Ollila HM, Peuralinna T, Myllykangas L, Kaivola K, Stone DJ, Traynor BJ, Renton AE, Rivera AM, Helisalmi S, Soininen H, Polvikoski T, Hiltunen M, Tienari PJ, Huttunen HJ and Paunio T (2018) Melatonin receptor type 1A gene linked to Alzheimer's disease in old age. *Sleep* **41**.

Sulkava S, Ollila HM, Alasaari J, Puttonen S, Harma M, Viitasalo K, Lahtinen A, Lindstrom J, Toivola A, Sulkava R, Kivimaki M, Vahtera J, Partonen T, Silander K, Porkka-Heiskanen T and Paunio T (2016) Common genetic variation near melatonin receptor 1A gene linked to job-related exhaustion in shift workers. *Sleep*.

Tice RR, Austin CP, Kavlock RJ and Bucher JR (2013) Improving the human hazard characterization of chemicals: a Tox21 update. *Environmental health perspectives* **121**:756-765.

Tischkau SA, Jaeger CD and Krager SL (2011) Circadian clock disruption in the mouse ovary in response to 2,3,7,8-tetrachlorodibenzo-p-dioxin. *Toxicology letters* **201**:116-122.

Tuomi T, Nagorny CL, Singh P, Bennet H, Yu Q, Alenkvist I, Isomaa B, Ostman B, Soderstrom J, Pesonen AK, Martikainen S, Raikkonen K, Forsen T, Hakaste L, Almgren P, Storm P, Asplund O, Shcherbina L, Fex M, Fadista J, Tengholm A, Wierup N, Groop L and Mulder H (2016) Increased Melatonin Signaling Is a Risk Factor for Type 2 Diabetes. *Cell Metab* **23**:1067-1077.

van der Westhuizen ET, Valant C, Sexton PM and Christopoulos A (2015) Endogenous allosteric modulators of G protein-coupled receptors. *The Journal of pharmacology and experimental therapeutics* **353**:246-260.

Wang HP, Liang YJ, Sun YJ, Hou WY, Chen JX, Long DX, Xu MY and Wu YJ (2014) Subchronic neurotoxicity of chlorpyrifos, carbaryl, and their combination in rats. *Environ Toxicol* **29**:1193-1200.

Whorton MD, Milby TH, Stubbs HA, Avashia BH and Hull EQ (1979) Testicular function among carbaryl-exposed exployees. *Journal of toxicology and environmental health* **5**:929-941.

Wyrobek AJ, Watchmaker G, Gordon L, Wong K, Moore D, 2nd and Whorton D (1981) Sperm shape abnormalities in carbaryl-exposed employees. *Environmental health perspectives* **40**:255-265.

Xia Y, Cheng S, Bian Q, Xu L, Collins MD, Chang HC, Song L, Liu J, Wang S and Wang X (2005) Genotoxic effects on spermatozoa of carbaryl-exposed workers. *Toxicological sciences : an official journal of the Society of Toxicology* **85**:615-623.

Xu CX, Krager SL, Liao DF and Tischkau SA (2010) Disruption of CLOCK-BMAL1 transcriptional activity is responsible for aryl hydrocarbon receptor-mediated regulation of Period1 gene. *Toxicological sciences : an official journal of the Society of Toxicology* **115**:98-108.

Xu CX, Wang C, Krager SL, Bottum KM and Tischkau SA (2013) Aryl hydrocarbon receptor activation attenuates Per1 gene induction and influences circadian clock resetting. *Toxicological sciences : an official journal of the Society of Toxicology* **132**:368-378.

Zheng T, Zahm SH, Cantor KP, Weisenburger DD, Zhang Y and Blair A (2001) Agricultural exposure to carbamate pesticides and risk of non-Hodgkin lymphoma. *Journal of occupational and environmental medicine* **43**:641-649.

Zirlik S, Hildner KM, Targosz A, Neurath MF, Fuchs FS, Brzozowski T and Konturek PC (2013) Melatonin and omentin: influence factors in the obstructive sleep apnoea syndrome? *Journal of physiology and pharmacology : an official journal of the Polish Physiological Society* **64**:353-360.

JPET Fast Forward. Published on November 17, 2020 as DOI: 10.1124/jpet.120.000065
This article has not been copyedited and formatted. The final version may differ from this version.

13. FOOTNOTES

a) Funding Information

This work was supported by Jacobs School of Medicine and Biomedical Sciences unrestricted funds (to MLD and RVR); National Institute of Health National Institute of Environmental Health Sciences [ES 023684 to MLD and RVR and ES 023684-S2 - Diversity Supplement to AJJ]; National Institute of Health National Institute of General Medical Sciences [GM 095459 to MLD; AJJ trainee]; PhRMA Foundation Fellowship [#73309 to AJJ trainee], and awards from the National Center for Advancing Translational Sciences to the University at Buffalo [UL1TR001412]. The research content is solely the responsibility of the authors and does not necessarily represent the official views of the NIH. No author has an actual or perceived conflict of interest with the contents of this article.

b) This work has previously been presented in part at

- **DUBOCOVICH, M.L.,** JONES, A., POPOVSKA-GOREVSKI, M., GLATFELTER, G., MASTANDREA, L.A., RAJNARAYANAN, R.V. Melatonin Receptors as Targets for Environmental Toxins Leading to Circadian Disruption and Risk for Diabetes. FASEB Summer Research Conference: Melatonin Receptors: Actions and Therapeutics. July 19-23, 2015, Lisbon, Portugal.
- **Glatfelter, G. C.**, Rajnarayanan, R. V., & Dubocovich, M. L. (April 2017). *Environmental Chemicals Compete for 2-[^{125}I]-Iodomelatonin Binding to Melatonin Receptors in Brain Slices from C3H/HeN Mice*. Experimental Biology

(EB): American Society for Pharmacology and Experimental Therapeutics (ASPET)

- **Glatfelter, G. C.**, Rajnarayanan, R. V., & Dubocovich, M. L. (April 2018). *Carbamate Insecticide Carbaryl Targets Melatonin Receptors and Modulates Circadian Rhythms*. Experimental Biology (EB): American Society for Pharmacology and Experimental Therapeutics (ASPET)
- **Jones, A.J.**, Mastrandrea L.D., Rajnarayanan R.V., & Dubocovich M.L. (April 2019). *Carbamate Insecticides Modulate G Protein-Dependent Signaling in Cells Expressing Melatonin Receptors*. Experimental Biology (EB): American Society for Pharmacology and Experimental Therapeutics (ASPET)
- **Glatfelter, G.C.**, Rajnarayanan, R. V., & Dubocovich, M. L. (April 2019) *Carbaryl Modulates Chronobiological Behaviors via Melatonin Receptors.* Experimental Biology (EB): American Society for Pharmacology and Experimental Therapeutics (ASPET)

c) For reprint request contact:
Margarita L. Dubocovich, Ph.D.
Department of Pharmacology and Toxicology
Jacobs School of Medicine and Biomedical Sciences
955 Main Street (Rm 3102)
University at Buffalo (SUNY)
Buffalo, NY 14203
Phone: 1-716-829-3048; Fax: 1-716-829-2801; Email: mdubo@buffalo.edu

JPET Fast Forward. Published on November 17, 2020 as DOI: 10.1124/jpet.120.000065
This article has not been copyedited and formatted. The final version may differ from this version.

d) Authorship Footnotes

[1] Co-First Authors - authors contributed equally

[2] Current address: Designer Drug Research Unit, National Institute of Drug Abuse Intramural Research Program, Baltimore, Maryland 21224, USA

[3] Current address: New York Institute of Technology at Arkansas State, Department of Basic Sciences and Arkansas Biosciences Institute, Jonesboro, AR 72467, USA

[4] To whom correspondence should be addressed:

Margarita L. Dubocovich, Ph.D.

Department of Pharmacology and Toxicology

Jacobs School of Medicine and Biomedical Sciences

955 Main Street (Rm 3102)

University at Buffalo (SUNY)

Buffalo, NY 14203

Phone: 1-716-829-3048; Fax: 1-716-829-2801; Email: mdubo@buffalo.edu

JPET Fast Forward. Published on November 17, 2020 as DOI: 10.1124/jpet.120.000065
This article has not been copyedited and formatted. The final version may differ from this version.

14. FIGURE LEGENDS

Figure 1. Structural similarity clustering of melatonin and carbamates. (A) Structures of melatonin and carbamates. (B) The carbamate insecticides carbaryl, carbofuran, bendiocarb, fenoxycarb, and fenobucarb cluster together and are structurally similar to melatonin. Normalized Tanimoto Index of chemical similarity in 2D and 3D are indicated as S_{2D} and S_{3D} respectively.

Figure 2. Molecular docking of melatonin and carbamate insecticides with human MT_1 and MT_2 melatonin receptors. Top docking poses of (A) melatonin (rendered in blue), (B) carbaryl (grey); (C) bendiocarb (yellow); (D) fenoxycarb (green), (E) fenobucarb (magenta) and (F) carbofuran (orange) with human MT_1 melatonin receptor. Cluster 1 carbamate insecticides (B-F) were able to bind to the putative melatonin binding pocket similar to the cognate ligand melatonin (A). (G-L) Molecular docking of melatonin and carbamate insecticides with human MT_2 melatonin receptor. Top docking poses of (G) melatonin (rendered in blue), (H) carbaryl (grey); (I) bendiocarb (yellow); (J) fenoxycarb (green), (K) fenobucarb (magenta) and (L) carbofuran (orange) with human MT_1 melatonin receptor. Cluster 1 carbamate insecticides (H-L) were able to bind to the putative melatonin binding pocket similar to the cognate ligand melatonin (G).

Figure 3. Carbamate insecticides compete for 2-[^{125}I]-iodomelatonin binding to hMT_1 and hMT_2 melatonin receptors. The ordinate represents 2-[^{125}I]-iodomelatonin binding expressed as percent total binding. Membranes from CHO cells stably expressing hMT_1 (A,B) or hMT_2 (C,D) melatonin receptors were incubated with 2-[^{125}I]-iodomelatonin (75 pM) in the absence (○) and the presence of various concentrations of ligands: (A,C) carbaryl (◆), fenoxycarb (□), and carbofuran (▲); (B,D) fenobucarb (◇), bendiocarb (■), and aldicarb (△). Symbols shown are the mean from representative experiments independently repeated three to eight times. See Table 1 for derived affinity constants.

JPET Fast Forward. Published on November 17, 2020 as DOI: 10.1124/jpet.120.000065
This article has not been copyedited and formatted. The final version may differ from this version.

Figure 4. Carbaryl binds to melatonin receptor orthosteric sites. The ordinates represent 2-[^{125}I]-iodomelatonin binding expressed as percent total 2-[^{125}I]-iodomelatonin binding to membranes from CHO cells stably expressing hMT_1 (A,C) or hMT_2 (B) melatonin receptors. Membranes were incubated with 2-[^{125}I]-iodomelatonin (■ = 30 pM, △ = 100 pM, ▼ = 300 pM, ◇ = 600 pM, ● = 1000 pM) and control or carbaryl (10 nM - 1 mM) in active (A,B) and resting buffer (C; + 100 μM GTP, 1 mM $EDTA.Na_2$, 150 mM NaCl). Symbols shown are the mean from representative experiments independently repeated three times. See Table S1 for derived binding constants (K_B) and cooperativity factors (α; α < 0.01, orthosteric; α ≥ 0.01, allosteric).

Figure 5. Carbamate insecticides compete for 2-[^{125}I]-iodomelatonin binding to hMT_1 and hMT_2 melatonin receptors without and with G protein inactivation. Membranes from CHO cells stably expressing hMT_1 (A) or hMT_2 (B) melatonin receptors were incubated with 2-[^{125}I]-iodomelatonin (75 pM) in the absence and the presence of various concentrations of melatonin (MLT), luzindole (LUZ), carbaryl† (CBRL), fenobucarb (FNBC), bendiocarb (BNDC), or carbofuran† (CBFN). † Denotes Ki values transformed from data obtained from Popovska-Gorevski, Dubocovich et al. 2017. See Supplemental Figure 4 for binding curves and Table 3 for derived affinity constants. (Left panels) The ordinate represents binding affinity in the absence (solid bars) and presence (dotted bars) of GTP expressed as pK_i. Connected points indicate values from simultaneously run experiments with the same tissue. (Right panels) The ordinate represents the mean differences in pK_i ($pK_{iGTP} - pK_{iControl} = \Delta pK_i$) and 95% confidence intervals produced by G protein inactivation. Ligands are classified as agonists (mean ΔpK_i below 20% MLT dashed-line), antagonists (mean ΔpK_i between 20% and -20% MLT dashed-lines), or inverse agonists (mean above -20% MLT dashed-line).

Figure 6. Representative autoradiograms show carbaryl competes *in vitro* for 2-[^{125}I]-iodomelatonin binding at melatonin receptors in slices containing the SCN, PVT, and PT from C3H/HeN WT mice. (A,B) Vehicle, melatonin (1 μM), or carbaryl (1,

JPET Fast Forward. Published on November 17, 2020 as DOI: 10.1124/jpet.120.000065
This article has not been copyedited and formatted. The final version may differ from this version.

10, 100 μM) treatments in representative magnified images taken from autoradiograms containing adjacent coronal sections containing the SCN and PVT (A) or PT (B) treated with 2-[^{125}I]-iodomelatonin (75 pM). Additional treatments are listed below in each section.

Figure 7. Quantitative receptor autoradiography demonstrates carbaryl competes *in vitro* for 2-[^{125}I]-iodomelatonin binding at melatonin receptors in slices containing the SCN, PVT, and PT from C3H/HeN mice. (A-F) Optical densities obtained for each treatment are normalized to percent total binding in the absence of drug treatment for each set of adjacent brain slices analyzed. Brain slices were treated with vehicle (VEH) or carbaryl (1, 10, 100 μM in vehicle) for 1 hour to assess competition for 2-[^{125}I]-iodomelatonin binding (75 pM) at melatonin receptors in slices containing the SCN, PVT, and PT. Dotted lines in each panel represent non-specific binding for adjacent slices treated with 1 μM melatonin for each data set. Comparison of treatment with carbaryl vs vehicle on % total binding from slices obtained from C3H WT mice (A-C), and MT_2KO mice (D-F). Values (n = 4-7 WT, n = 2-7 MT_2KO) in each panel are compared to % total binding of vehicle-treated slices using a one-way ANOVA with Dunnet's post-test ($P < 0.05$). *$P < 0.05$, ***$P < 0.001$, ****$P < 0.0001$. See Table 2 & Supplemental Table 5 for derived affinity constants. See Supplemental Table 3 for additional information regarding descriptive statistics and data comparisons.

Figure 8. Carbaryl competes *ex vivo* for 2-[^{125}I]-iodomelatonin binding at melatonin receptors in slices containing the SCN, PVT, and PT from C3H/HeN WT mice. Specific binding of 2-[^{125}I]-iodomelatonin (50 pM) *ex vivo* in the SCN (A), PVT (B), or PT (C) of brain slices quantified at 0, 30, 60, 120, and 240 minutes post *in vivo* administration of vehicle (VEH) or carbaryl (10 mg/kg i.p. in vehicle). Values (n = 3 - 6) are compared to VEH (n = 10) using a one-way ANOVA with Dunnet's post-test ($P < 0.05$). Specific binding was determined by subtracting non-specific values from adjacent slices treated with only the radioligand. *$P < 0.05$, **$P < 0.01$, ****$P < 0.0001$.

JPET Fast Forward. Published on November 17, 2020 as DOI: 10.1124/jpet.120.000065
This article has not been copyedited and formatted. The final version may differ from this version.

Figure 9. Carbaryl phase advances running wheel activity onset after 3 days of injections at CT 10 similar to melatonin. Representative running wheel activity actograms from C3H/HeN mice treated with vehicle (A; saline 15% EtOH i.p. n = 7), carbaryl (B; 10 mg/kg i.p. n = 12), or melatonin (C; 3 mg/kg, s.c. n = 4) for 3 consecutive days indicated by the black dots. Carbaryl ($P < 0.001$) and melatonin ($P < 0.001$) produced a significant phase advance compared to vehicle (D; $F_{2,20} = 29.59$, $P < 0.001$). *** $P < 0.001$

JPET Fast Forward. Published on November 17, 2020 as DOI: 10.1124/jpet.120.000065
This article has not been copyedited and formatted. The final version may differ from this version.

15. TABLES

Table 1. Competition of carbamate insecticides for 2-[^{125}I]-iodomelatonin binding to hMT_1 or hMT_2 melatonin receptors expressed in CHO cells.

Ligand	Ligand Competition for 2-[^{125}I]-Iodomelatonin Binding				
	Human MT_1		Human MT_2		Ratio
	pK_i	n	pK_i	n	$K_{i\ hMT1}$ / $K_{i\ hMT2}$
Carbaryl	5.52 (5.29 - 5.75)	6	6.81 (6.65 - 6.96)	6	20
Fenobucarb	5.01 (4.89 - 5.13)	6	6.27 (6.16 - 6.38)	6	18
Fenoxycarb	4.53 (4.41 - 4.66)	8	4.55 (4.40 - 4.70)	5	1.1
Bendiocarb	4.38 (4.30 - 4.45)	5	5.53 (5.40 - 5.67)	6	14
Carbofuran	4.03 (3.91 - 4.14)	3	5.46 (5.12 - 5.80)	3	26
Oxamyl	3.59 (3.04 - 4.15)	3	3.99 (3.60 - 4.48)	3	2.6
Aldicarb	3.29 (2.88 - 3.70)	3	5.01 (4.90 - 5.12)	3	55
Methomyl	3.01 (2.43 - 3.60)	3	3.38 (2.96 - 3.81)	3	2.4

Competition of various carbamates insecticides (10 nM to 10 mM) for 2-[^{125}I]-iodomelatonin (75 pM) binding to hMT_1 or hMT_2 melatonin receptors stably expressed in CHO cells. pKi values were calculated from IC_{50} values obtained from competition curves (see Fig. 3) by the method of Cheng and Prusoff (1973). Shown are mean pKi

JPET Fast Forward. Published on November 17, 2020 as DOI: 10.1124/jpet.120.000065
This article has not been copyedited and formatted. The final version may differ from this version.

values and 95% confidence intervals of at least 3 independent determinations. K_i ratios represent fold difference ($K_{i(hMT1)}/K_{i(hMT2)}$) in affinity of each carbamate insecticide for hMT_1 and hMT_2 melatonin receptors. pK_i values for melatonin are 9.84 (95% CI = 9.55 to 10.14; n = 5) at the hMT_1 and 9.65 (95% CI = 9.53 to 9.76; n = 5) at the hMT_2 ($K_{i(hMT1)}/K_{i(hMT2)} = 0.70$).

JPET Fast Forward. Published on November 17, 2020 as DOI: 10.1124/jpet.120.000065
This article has not been copyedited and formatted. The final version may differ from this version.

Table 2. Affinity constants of carbamate insecticides compete for 2-[^{125}I]-iodomelatonin binding to SCN, PVT, and PT in brain slices from C3H/HeN mice.

Ligand	Competition for 2-[^{125}I]-Iodomelatonin Binding *In vitro*			
	hMT_1 CHO	Mouse SCN	Mouse PVT	Mouse PT
	pK_i	pK_i	pK_i	pK_i
Carbaryl	5.52 (5.29 - 5.75)	5.50 (5.30 - 5.71)	5.51 (5.03 - 5.98)	5.10 (4.76 - 5.44)
Fenobucarb	5.01 (4.89 - 5.13)	4.93 (4.27 - 5.58)	5.18 (4.59 - 5.78)	6.17 (2.36 - 9.97)
Bendiocarb	4.38 (4.30 - 4.45)	4.74 (3.70 - 5.77)	4.41 (4.07 - 4.76)	3.70 (3.39 - 4.00)

Carbaryl, fenobucarb, and bendiocarb (1-100 □M) competed for 2-[^{125}I]-iodomelatonin (75 pM) binding to melatonin receptors in SCN, PVT, and PT C3H/HeN mouse brain slices as determined by quantitative receptor autoradiography. K_i values were determined by the method of Cheng and Prusoff (1973) were used to calculate pK_i values. Shown are mean pK_i values and 95% confidence intervals from independent determinations: SCN (n = 3-7), PVT (n = 3-7), and PT (n = 2-4). pK_i for hMT_1 expressed in CHO cells is shown for comparison (Table 1, Figure 3).

Table 3. Competition of melatonin, luzindole, and cluster 1-carbamate insecticides for 2-[^{125}I]-iodomelatonin binding to hMT_1 and hMT_2 expressed in CHO cells without and with G protein inactivation.

Ligand	Ligand Competition for 2-[^{125}I]-Iodomelatonin Binding							
	Human MT_1				Human MT_2			
	pK_i		$\Delta pK_{i(GTP-Ctrl)}$	n	pK_i		$\Delta pK_{i(GTP-Ctrl)}$	n
	Control	GTP			Control	GTP		
Melatonin	9.84 (9.55 - 10.1)	8.65 (8.50 - 8.80)	-1.19*** (-1.56 - 0.83)	5	9.65 (9.53 - 9.76)	9.23 (9.10 - 9.36)	-0.41** (-0.62 - -0.21)	5
Luzindole	6.52 (6.33 - 6.71)	7.20 (6.96 - 7.44)	0.68* (0.26 - 1.10)	3	7.97 (7.67 - 8.28)	7.77 (7.35 - 8.18)	-0.21 (-0.66 - 0.24)	4
Carbaryl†	5.22 (4.94 - 5.51)	5.36 (5.20 - 5.45)	0.10 (-0.09 - 0.30)	5	6.99 (6.76 - 7.21)	6.17 (5.97 - 6.36)	-0.82*** (-0.92 - -0.72)	5
Fenobucarb	4.92 (4.55 - 5.29)	4.72 (4.58 - 4.86)	-0.20 (-0.46 - 0.06)	3	6.24 (5.89 - 6.59)	5.38 (5.18 - 5.59)	-0.85** (-1.02 - -0.68)	3
Bendiocarb	4.41 (4.24 - 4.58)	4.27 (4.05 - 4.50)	-0.13 (-0.48 - 0.21)	3	5.60 (5.25 - 5.94)	4.79 (4.75 - 4.83)	-0.81** (-1.14 - -0.47)	3
Carbofuran†	3.85 (3.62 - 4.08)	3.93 (3.71 - 4.15)	0.08 (-0.18 - 0.33)	5	5.64 (5.42 - 5.86)	4.71 (4.40 - 5.02)	-0.93*** (-1.16 - -0.71)	5

Competition for 2-[^{125}I]-iodomelatonin (75 pM) binding of melatonin, luzindole, and cluster 1-carbamate insecticides were performed in the absence (active buffer) or presence (resting buffer) of 100 µM GTP, 1 mM $EDTA.Na_2$ and 150 mM NaCl at 25°C for 1 hour. pKi values were calculated from IC_{50} values obtained from competition curves (See Fig. S4) by the

method of Cheng and Prusoff (1973). Shown are mean pKi values and 95% confidence intervals of at least 3 independent determinations. pK_is obtained in active and resting buffer were analyzed for differences using two-tailed paired *t* tests. ($^{*}P < 0.05$; $^{**}P < 0.01$; $^{***}P < 0.001$). Decreases ($\Delta pK_i = pK_{iGTP} - pK_{iControl}$; negative ΔpK_i and > 20% MLT effect) of affinity in resting buffer indicates agonist apparent efficacy while no change or increases in affinity (< 20% MLT effect or positive ΔpK_i) indicates antagonist or inverse agonist apparent efficacy, respectively. † Denotes Ki values transformed from data obtained from Popovska-Gorevski, Dubocovich et al. 2017.

JPET Fast Forward. Published on November 17, 2020 as DOI: 10.1124/jpet.120.000065
This article has not been copyedited and formatted. The final version may differ from this version.

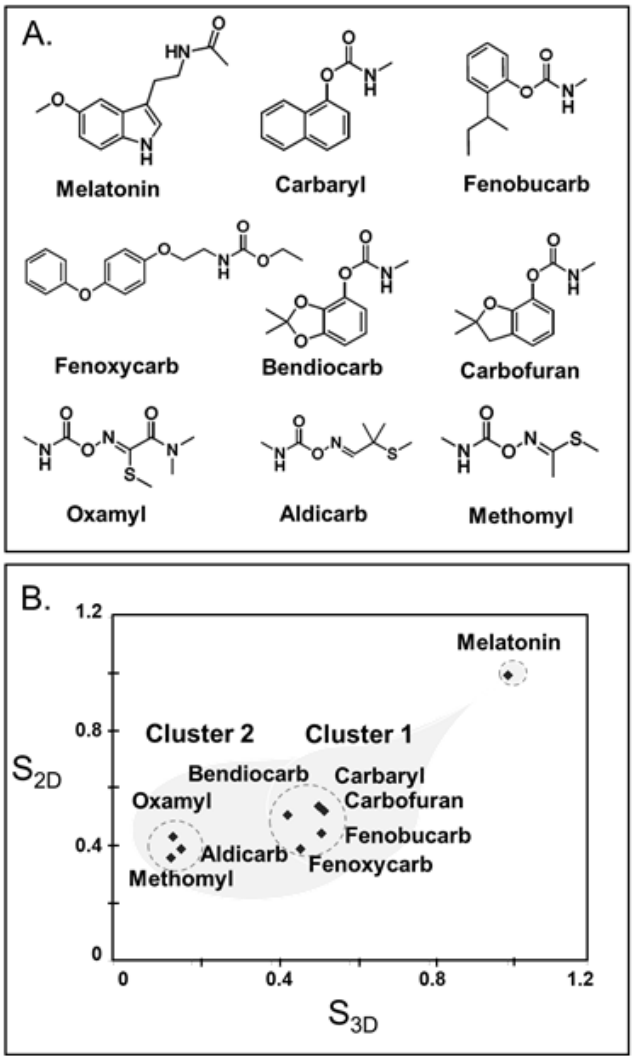

Figure 1

JPET Fast Forward. Published on November 17, 2020 as DOI: 10.1124/jpet.120.000065
This article has not been copyedited and formatted. The final version may differ from this version.

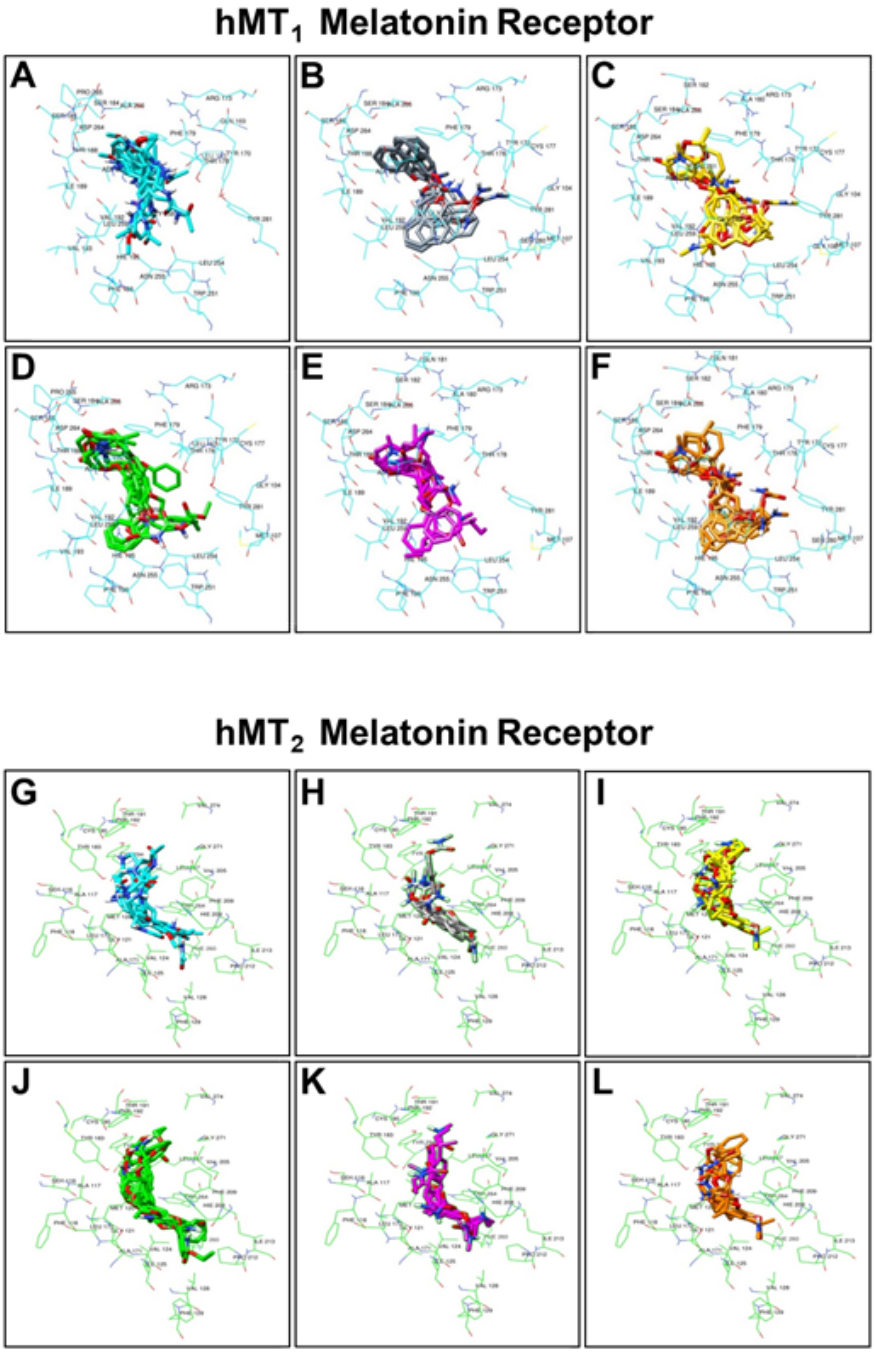

Figure 2

JPET Fast Forward. Published on November 17, 2020 as DOI: 10.1124/jpet.120.000065
This article has not been copyedited and formatted. The final version may differ from this version.

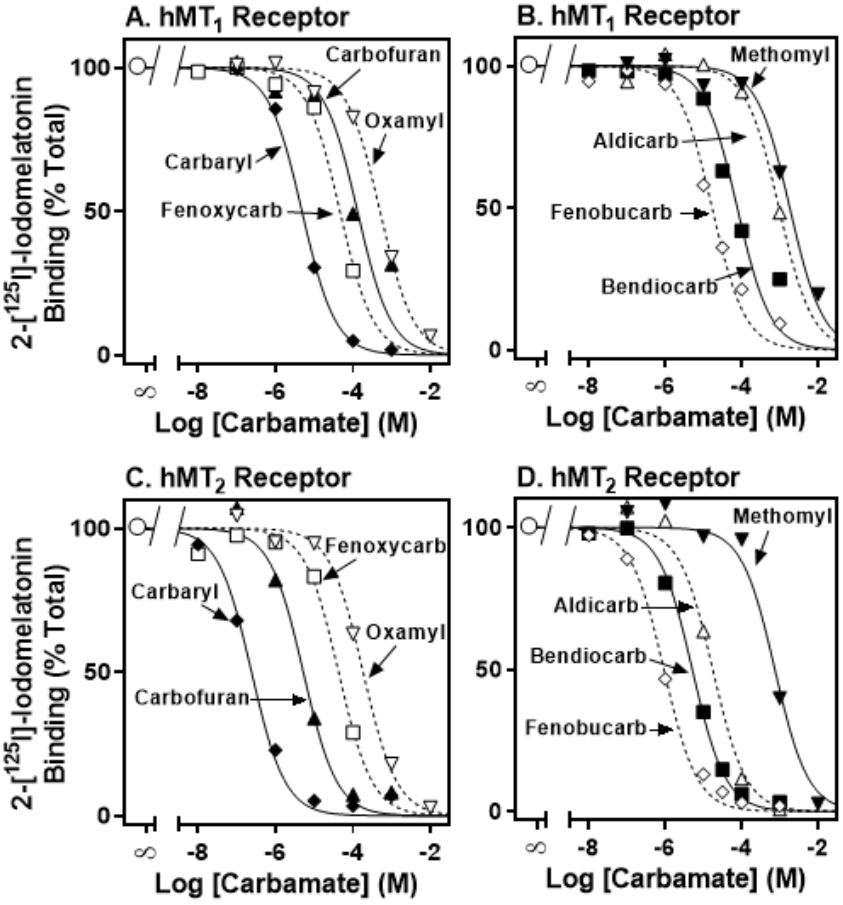

Figure 3

JPET Fast Forward. Published on November 17, 2020 as DOI: 10.1124/jpet.120.000065
This article has not been copyedited and formatted. The final version may differ from this version.

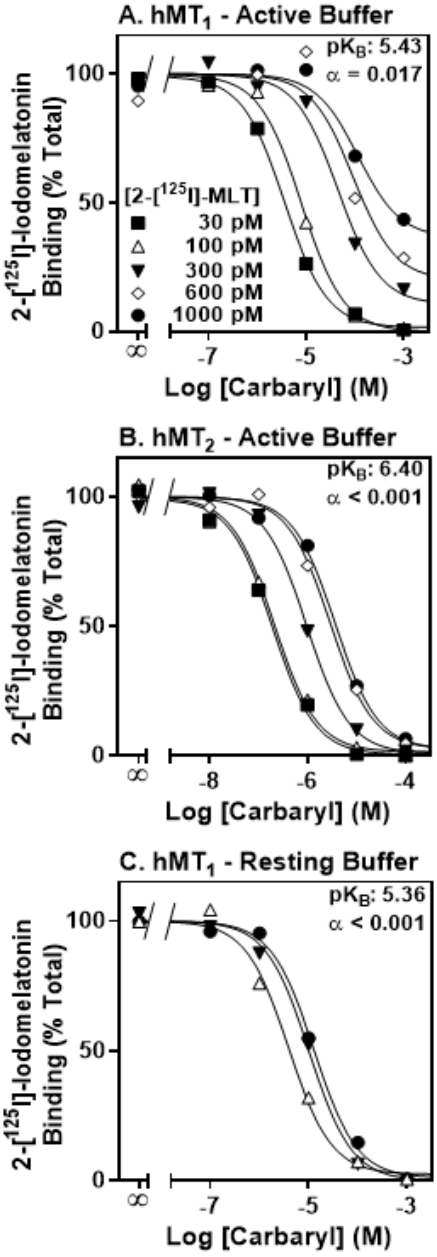

Figure 4

JPET Fast Forward. Published on November 17, 2020 as DOI: 10.1124/jpet.120.000065
This article has not been copyedited and formatted. The final version may differ from this version.

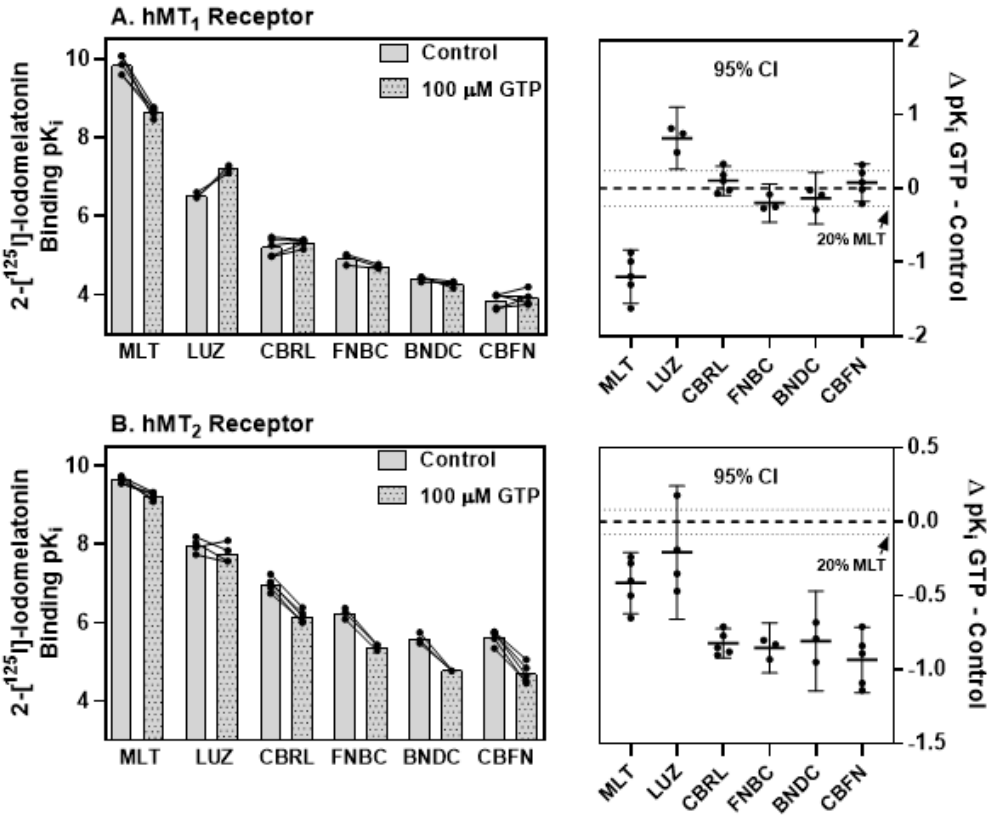

Figure 5

JPET Fast Forward. Published on November 17, 2020 as DOI: 10.1124/jpet.120.000065
This article has not been copyedited and formatted. The final version may differ from this version.

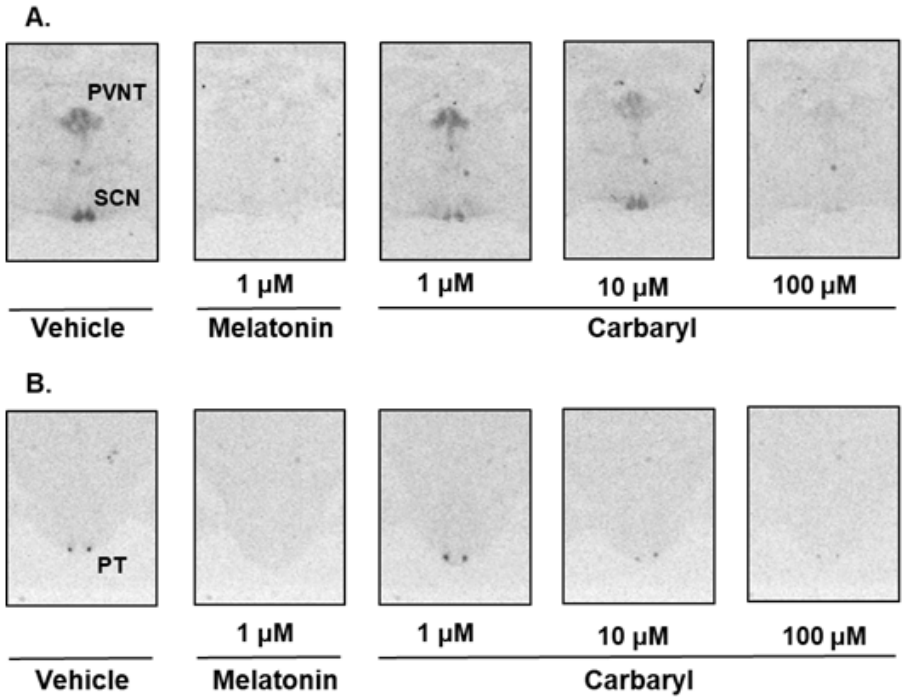

Figure 6

JPET Fast Forward. Published on November 17, 2020 as DOI: 10.1124/jpet.120.000065
This article has not been copyedited and formatted. The final version may differ from this version.

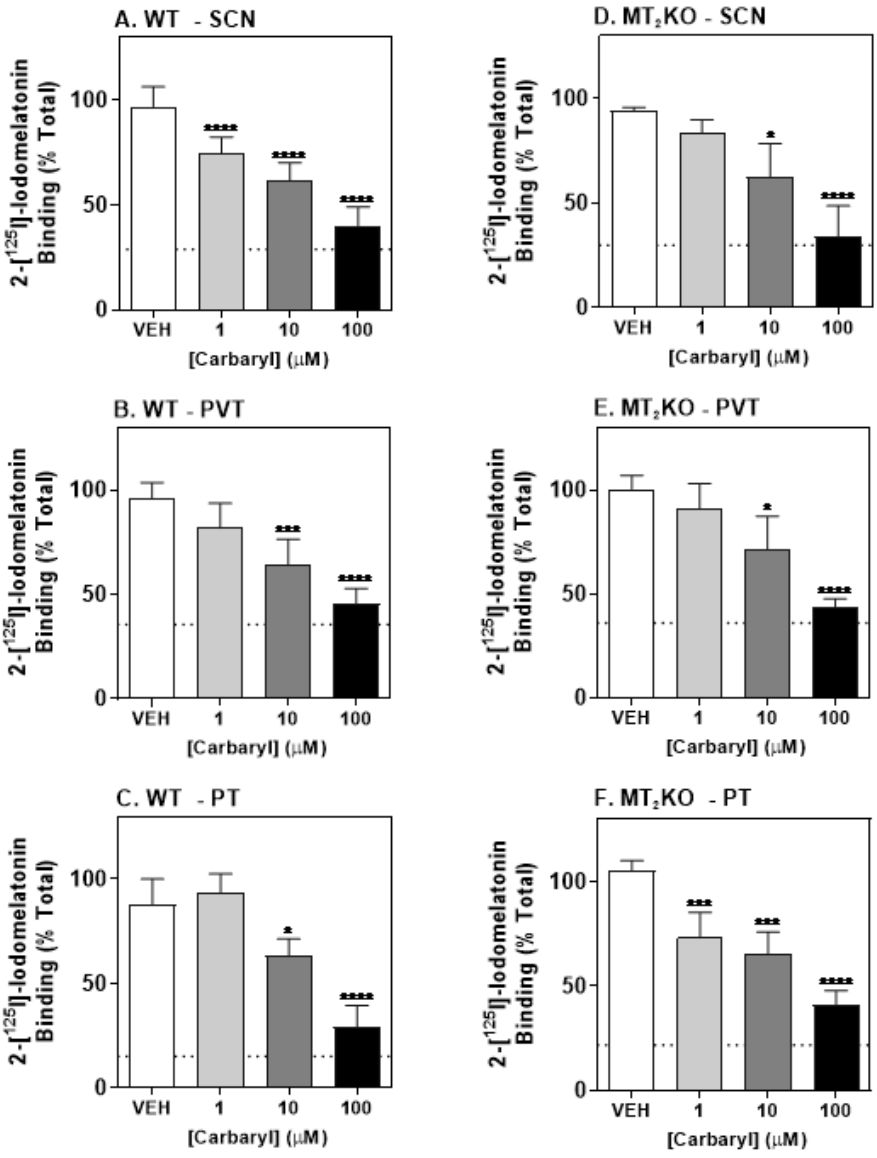

Figure 7

JPET Fast Forward. Published on November 17, 2020 as DOI: 10.1124/jpet.120.000065
This article has not been copyedited and formatted. The final version may differ from this version.

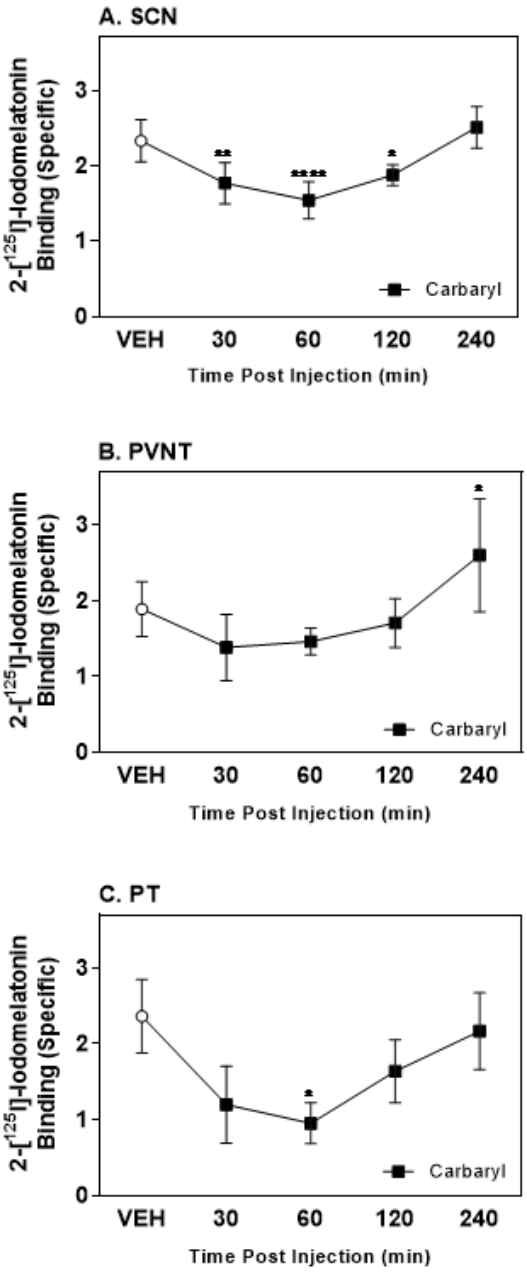

Figure 8

JPET Fast Forward. Published on November 17, 2020 as DOI: 10.1124/jpet.120.000065
This article has not been copyedited and formatted. The final version may differ from this version.

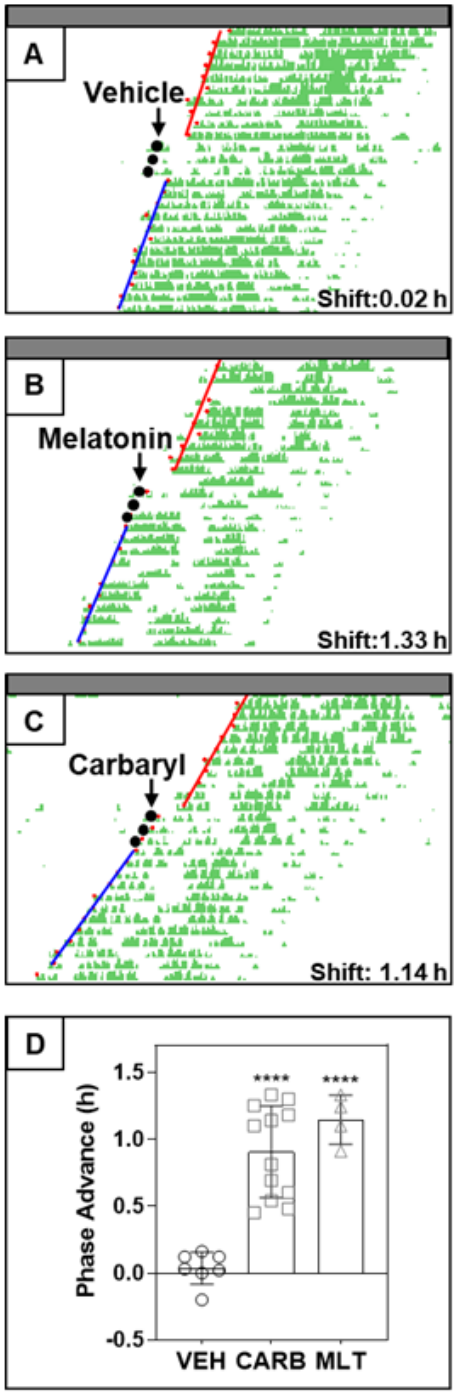

Figure 9

Supplemental Tables & Figures

Pharmacological Actions of Carbamate Insecticides at Mammalian Melatonin Receptors

Grant C. Glatfelter [1,2], Anthony J. Jones [1], Rajendram V. Rajnarayanan [3], and Margarita L. Dubocovich [4]

Department of Pharmacology & Toxicology (G.C.G., A.J.J., R.V.R., M.L.D.), Interdepartmental Neuroscience Program (A.J.J., M.L.D.), Jacobs School of Medicine and Biomedical Sciences - University at Buffalo, Buffalo, NY 14203.

Submitted to Journal of Pharmacology and experimental Therapeutics (JPET)

18. SUPPLEMENTAL DATA

Supplemental Table 1. Binding affinity values and cooperativity factors for melatonin, luzindole, and carbaryl at hMT_1 and hMT_2 melatonin receptors expressed in CHO cells.

Ligand	Ligand Competition for 2-[^{125}I]-Iodomelatonin Binding					
	Human MT_1 (A)		Human MT_1 (R)		Human MT_2 (A)	
	pK_B	α	pK_B	α	pK_B	α
Melatonin	9.71 (9.09 - 10.3)	< 0.001	N.D.	N.D.	9.91 (9.68 - 10.2)	< 0.001
Luzindole	6.41 (6.27 - 6.56)	0.037 (0.003 - 0.093)	7.27 (7.15 - 7.39)	< 0.001	7.87 (7.65 - 8.08)	< 0.001
Carbaryl	5.43 (5.15 - 5.71)	0.017 (0.012 - 0.022)	5.36 (5.19 - 5.53)	< 0.001	6.40 (5.76 - 7.04)	< 0.001

Equilibrium binding constants (K_B) and cooperativity factors (α) for melatonin, luzindole, and carbaryl at hMT_1 and hMT_2 melatonin receptors stably expressed in CHO cells in active (A) or resting (R) buffer (+ 100 µM GTP, 1 mM EDTA.Na_2, 150 mM NaCl), were determined by ligand competition for various concentrations (30 -1400 pM) of 2-[^{125}I]-iodomelatonin. Radioligand concentration, IC_{50}, and maximal fractional inhibition obtained from binding curves (see Figs. 4 and S2) were used to calculate pK_B and α values (Cheng and Prusoff 1973, Lazareno and Birdsall 1995). Shown are mean pK_B and α values with 95% confidence intervals from 3 independent experiments. α < 0.01 reveals an orthosteric binding mechanism while α ≥ 0.01 indicates allosteric binding.

Supplemental Table 2. 2-[^{125}I]-Iodomelatonin binding dissociation rates from hMT_1 and hMT_2 melatonin receptors in the absence and presence of luzindole or cluster 1-carbamate insecticides.

Test Compound	2-[^{125}I]-Iodomelatonin Dissociation Binding			
	Human MT_1 (R)		Human MT_2 (R)	
	K_{off} (min^{-1})	$\Delta K_{off\ (Veh-Test)}$ (min^{-1})	K_{off} (min^{-1})	$\Delta K_{off\ (Veh-Test)}$ (min^{-1})
Vehicle	0.437 (0.366 - 0.507)	N/A	0.0827 (0.0551 - 0.110)	N/A
Luzindole	0.402 (0.358 - 0.446)	0.0345 (-0.0179 - 0.0869)	0.0890 (0.0420 - 0.136)	-0.00635 (-0.0337 - 0.0210)
Carbaryl	0.421 (0.316 - 0.527)	0.0152 (-0.0115 - 0.145)	0.0777 (0.0444 - 0.111)	0.00503 (-0.00317 - 0.132)
Fenobucarb	0.437 (0.366 - .509)	-0.0008 (-0.130 - 0.128)	0.0791 (0.0411 - 0.117)	0.00359 (-0.0120 - 0.0191)
Bendiocarb	0.447 (0.339 - 0.555)	0.0104 (-0.157 - 0.136)	0.0814 (0.0495 - 0.113)	0.00133 (-0.0109 - 0.0136)
Carbofuran	0.470 (0.356 - 0.584)	-0.0335 (-0.166 - 0.0992)	0.0796 (0.0543 - 0.105)	0.00310 (-0.0234 - 0.0296)

Dissociation rates (K_{off}) of 2-[^{125}I]-iodomelatonin (100 pM) binding to CHO-hMT_1 or CHO-hMT_2 membranes in resting buffer (R), initiated by challenge with 10 μM melatonin in the absence (vehicle) or the presence of 100 μM luzindole, carbaryl, fenobucarb, bendiocarb, or carbofuran (see Fig. S3). Shown are mean K_{off} values and 95% confidence intervals of 3 independent experiments run in duplicate. Mean difference in dissociation rates (with 95% CI) between vehicle and test compounds (ΔK_{off}) are also reported for comparison by Friedman test (MT_1: $P = 0.043$; MT_2: $P = 0.74$) with Dunn's post-test for multiple comparisons ($P > 0.05$ for all comparisons).

Supplemental Table 3. Additional information regarding descriptive statistics and analyses for Fig. 7, Fig. 8, & Fig. 9.

	Post-hoc Test Comparisons (all α = 0.05)						
Figure	Control	mean ± SD	*n*	Treatment	mean ± SD	*n*	*P*-value *P* =
7a	Total + Vehicle	97.03 ± 9.54	4	1 μM	74.69 ± 7.83	7	**0.0011**
SCN				10 μM	61.95 ± 8.30	7	**< 0.0001**
WT	1 μM Melatonin	28.92 ± 10.47	7	100 μM	40.16 ± 8.83	7	**< 0.0001**
7b	Total + Vehicle	96.12 ± 7.37	4	1 μM	81.76 ± 11.90	7	**0.0821**
PVT				10 μM	64.41 ± 12.00	7	**0.0002**
WT	1 μM Melatonin	35.48 ± 9.69	7	100 μM	45.53 ± 7.25	7	**< 0.0001**
7c	Total + Vehicle	87.77 ± 12.25	4	1 μM	93.58 ± 8.94	4	0.7498
PT				10 μM	63.55 ± 7.83	4	**0.0127**
WT	1 μM Melatonin	15.10 ± 6.51	4	100 μM	29.21 ± 10.21	4	**< 0.0001**
7d	Total + Vehicle	94.05 ± 1.75	2	1 μM	83.91 ± 5.97	7	0.5403
SCN				10 μM	62.32 ± 16.02	7	**0.0123**
MT_2KO	1 μM Melatonin	29.87 ± 4.88	7	100 μM	34.00 ± 14.68	7	**< 0.0001**
7e	Total + Vehicle	100.4 ± 6.58	2	1 μM	91.19 ± 11.74	7	0.5630
PVT				10 μM	71.46 ± 15.91	7	**0.0151**
MT_2KO	1 μM Melatonin	36.05 ± 8.01	7	100 μM	43.62 ± 4.06	7	**< 0.0001**
7f	Total + Vehicle	105.3 ± 4.97	4	1 μM	73.19 ± 12.15	4	**0.0009**
PT				10 μM	65.46 ± 10.51	4	**0.0001**
MT_2KO	1 μM Melatonin	21.71 ± 1.94	4	100 μM	40.86 ± 6.97	4	**< 0.0001**
8a	Vehicle	2.33 ± 0.28	10	30 mins	1.77 ± 0.27	5	**0.0021**
SCN				60 mins	1.54 ± 0.25	6	**< 0.0001**
				120 mins	1.88 ± 0.14	4	**0.0236**
				240 mins	2.51 ± 0.28	3	0.7196
8b	Vehicle	1.89 ± 0.36	10	30 mins	1.38 ± 0.44	5	0.0943
PVT				60 mins	1.46 ± 0.18	6	0.1545
				120 mins	1.71 ± 0.32	4	0.8763
				240 mins	2.59 ± 0.74	3	**0.0403**
8c	Vehicle	2.36 ± 0.48	3	30 mins	1.20 ± 0.51	2	0.0908
PT				60 mins	0.95 ± 0.27	2	**0.0439**
				120 mins	1.64 ± 0.42	2	0.3434
				240 mins	2.17 ± 0.51	2	0.9700
9d	Vehicle	0.04 ± 0.12	7	Carbaryl	0.91 ± 0.34	12	**< 0.0001**
				Melatonin	1.15 ± 0.18	4	**< 0.0001**

Summary table describing details of statistical analyses and descriptive statistics. Alpha set *at P* < 0.05 for all analyses using Dunnett's post-test compared to total + vehicle (7A-F) or vehicle (8A-C, 9D). Bolded *P*-values represent significant results. Further details on statistical testing and experimental details for each figure (Fig 7, Fig. 8, Fig.9) found in corresponding figure legends or **Materials & Methods** section. Main effects and other statistical details as appropriate for each data set are reported in corresponding figure legends (Fig 7, Fig. 8, Fig.9) or **Results**.

Supplemental Table 4. Additional information regarding descriptive statistics and analyses for Supplemental Fig. 5 quantitative receptor autoradiography results.

				Post-hoc Test Comparisons (all α = 0.05)				
Figure	Control	mean ± SD	*n*	Treatment	Concentration	mean ± SD	*n*	*P*-value *P* =
Supp. 5a	Total + Vehicle	101.7 ± 2.93	3		1 μM	99.65 ± 6.49	3	0.9799
SCN				Bendiocarb	10 μM	89.73 ± 4.57	2	0.3245
WT	1 μM Melatonin	36.98 ± 2.49	3		100 μM	54.95 ± 13.00	3	**0.0005**
Supp. 5b	Total + Vehicle	102.3 ± 3.99	3		1 μM	109.4 ± 7.49	3	0.3274
PVT				Bendiocarb	10 μM	94.84 ± 0.16	2	0.3639
WT	1 μM Melatonin	45.14 ± 4.46	3		100 μM	68.52 ± 5.36	3	**0.0003**
Supp. 5c	Total + Vehicle	91.67 ± 6.92	2		1 μM	84.37 ± 14.57	2	0.8540
PT				Bendiocarb	10 μM	82.32 ± 11.49	2	0.7556
WT	1 μM Melatonin	16.34 ± 3.29	2		100 μM	40.32 ± 10.62	2	**0.0233**
Supp. 5d	Total + Vehicle	111.8 ± 16.89	3		1 μM	86.66 ± 18.62	3	0.9857
SCN				Fenobucarb	10 μM	62.32 ± 16.02	3	0.1486
WT	1 μM Melatonin	32.70 ± 0.88	3		100 μM	36.14 ± 4.95	3	**0.0005**
Supp. 5e	Total + Vehicle	99.86 ± 14.84	3		1 μM	95.22 ± 5.59	3	0.9114
PVT				Fenobucarb	10 μM	72.15 ± 11.06	3	**0.0337**
WT	1 μM Melatonin	31.85 ± 4.22	3		100 μM	31.82 ± 9.53	3	**0.0002**
Supp. 5f	Total + Vehicle	97.03 ± 15.91	2		1 μM	59.95 ± 12.43	2	0.0598
PT				Fenobucarb	10 μM	45.92 ± 2.39	2	**0.0210**
WT	1 μM Melatonin	22.86 ± 4.01	2		100 μM	23.61 ± 7.63	2	**0.0057**

Summary table describing details of statistical analyses and descriptive statistics. Alpha set *at P* < 0.05 for all analyses using Dunnett's post-test compared to total + vehicle. Non-specific binding by melatonin is shown in each data set for reference. Bolded *P*-values represent significant results. Further details on statistical testing and experimental details for each figure (Supplemental Fig. 5A, B, C for bendiocarb and D, E, F for fenobucarb) found in corresponding figure legends or **Materials & Methods**. Main effects and other details as appropriate for each data set are reported in corresponding figure legends or **Results**.

Supplemental Table 5. Affinity constants of carbaryl for 2-[^{125}I]-iodomelatonin binding to SCN, PVT, and PT in brain slices from C3H/HeN WT & MT_2KO mice.

Genotype	Competition for 2-[^{125}I]-Iodomelatonin Binding		
	Mouse SCN	Mouse PVT	Mouse PT
	pK_i	pK_i	pK_i
Carbaryl WT	5.50 (5.30 - 5.71)	5.51 (5.03 - 5.98)	5.10 (4.76 - 5.44)
Carbaryl MT_2KO	5.38 (4.99 - 5.77)	5.23 (4.93 - 5.52)	5.29 (4.42 - 6.12)

Carbaryl (1-100 μM) competed for 2-[^{125}I]-iodomelatonin (75 pM) binding to melatonin receptors in SCN, PVT, and PT C3H/HeN mouse brain slices as determined by quantitative receptor autoradiography. pK_i values were calculated from K_i values determined by the method of Cheng and Prusoff (1973). Shown are mean pK_i values and 95% confidence intervals from *n* = 4-7 independent determinations. Values for WT mice are also appear in Table 2.

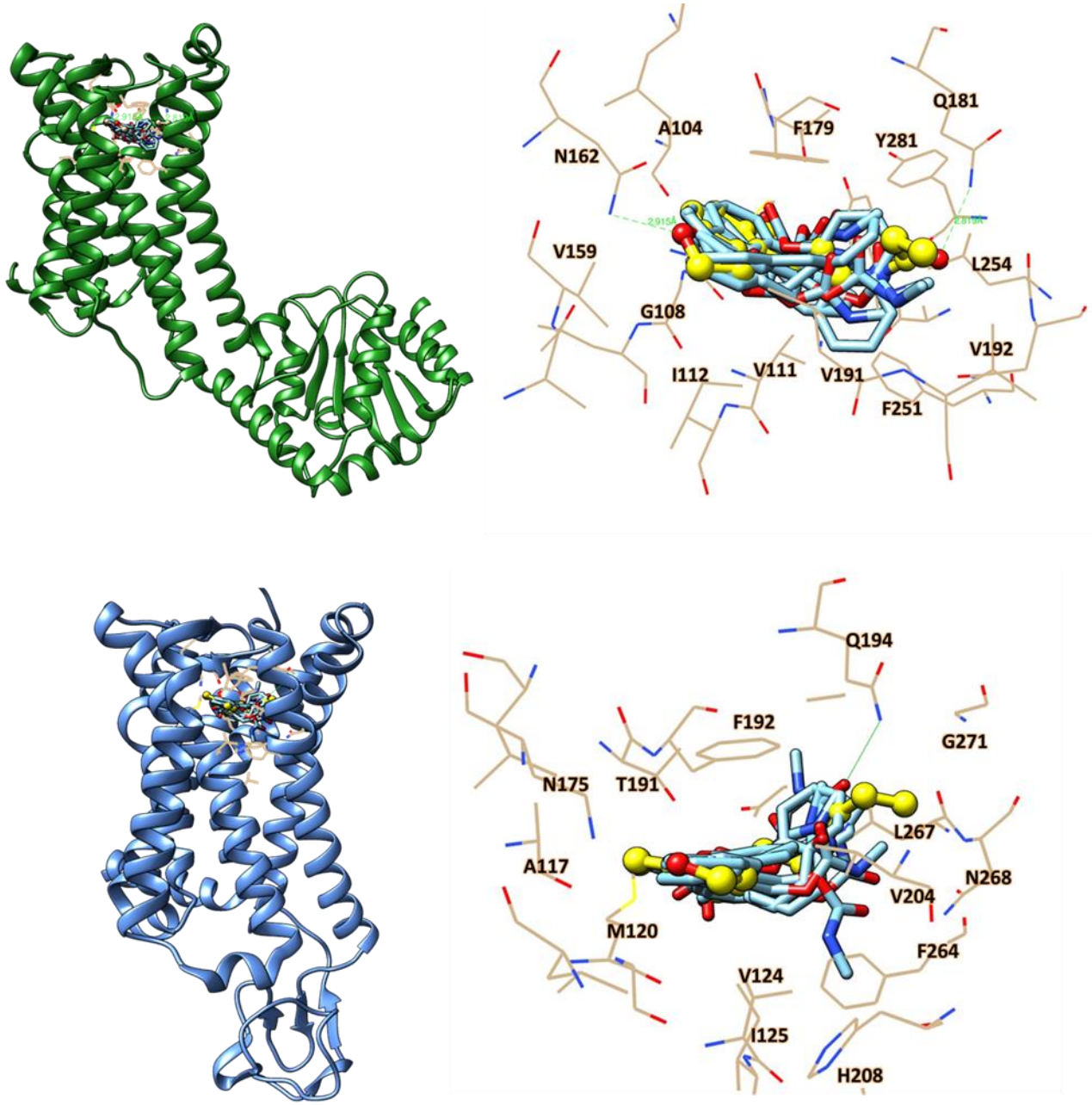

Supplemental Figure 1. Molecular docking of carbaryl with human MT_1 and MT_2 melatonin receptor models derived from X-ray crystal structures. MT_1 (A; rendered in green; PDB ID: 6ME2) and MT_2 (B; blue; PDB ID: 6ME9) melatonin receptors in complex with ramelteon (yellow) with top 5 docked poses of carbaryl (cyan). Carbaryl

bound to the putative MT_1-melatonin binding pocket like the cognate ligand ramelteon, however at the MT_2-melatonin binding pocket, carbaryl and ramelteon displayed dissimilar interactions.

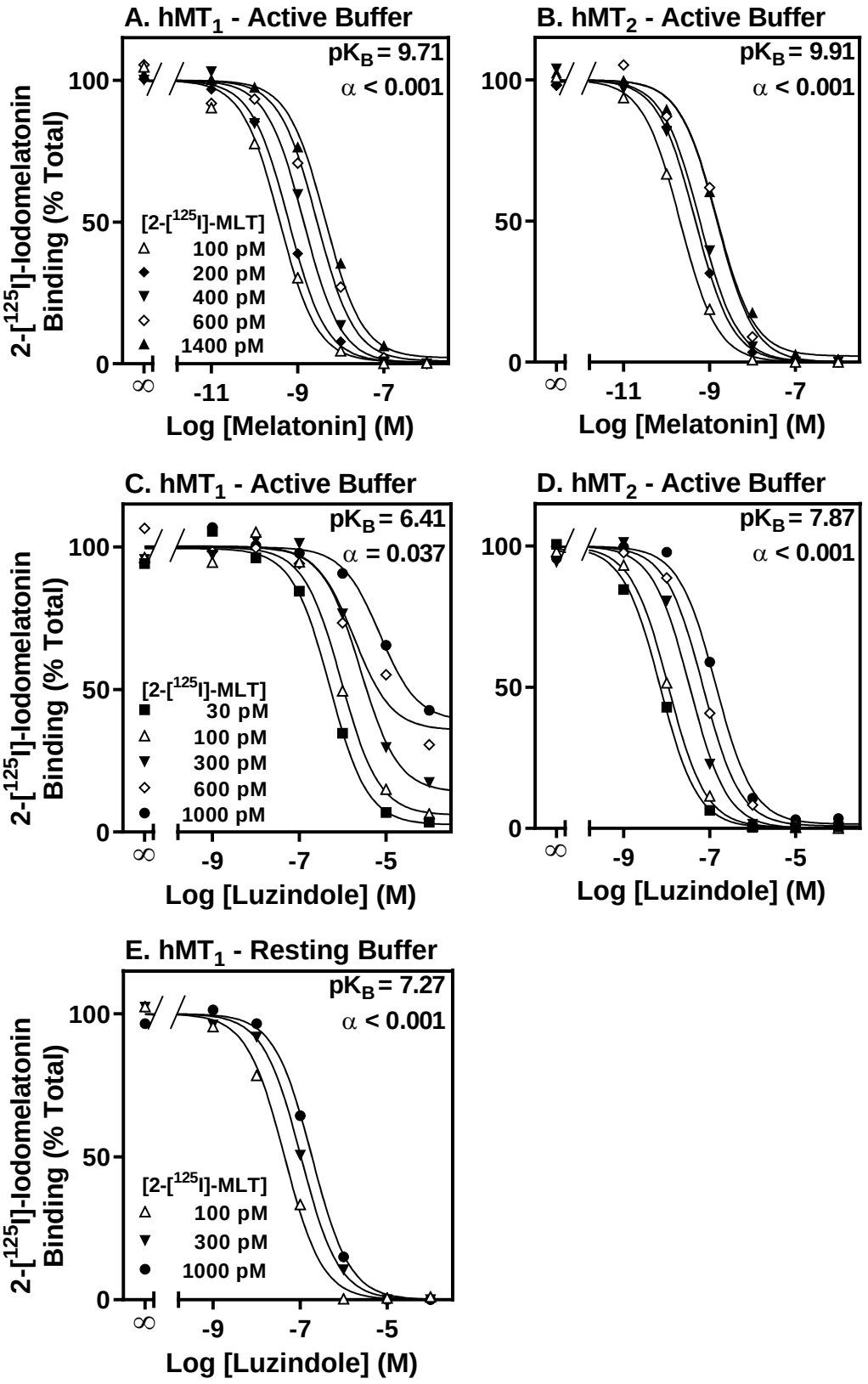
A. hMT1 - Active Buffer
pKB = 9.71
α < 0.001
[2-[125I]-MLT]
100 pM
200 pM
400 pM
600 pM
1400 pM
2-[125I]-Iodomelatonin Binding (% Total)
Log [Melatonin] (M)
B. hMT2 - Active Buffer
pKB = 9.91
α < 0.001
Log [Melatonin] (M)
C. hMT1 - Active Buffer
pKB = 6.41
α = 0.037
[2-[125I]-MLT]
30 pM
100 pM
300 pM
600 pM
1000 pM
2-[125I]-Iodomelatonin Binding (% Total)
Log [Luzindole] (M)
D. hMT2 - Active Buffer
pKB = 7.87
α < 0.001
Log [Luzindole] (M)
E. hMT1 - Resting Buffer
pKB = 7.27
α < 0.001
[2-[125I]-MLT]
100 pM
300 pM
1000 pM
2-[125I]-Iodomelatonin Binding (% Total)
Log [Luzindole] (M)

Supplemental Figure 2. Characterization of 2-[^{125}I]-iodomelatonin binding mechanism for melatonin and luzindole. The ordinates represent 2-[^{125}I]-iodomelatonin binding expressed as percent total 2-[^{125}I]-iodomelatonin binding to membranes from CHO cells stably expressing hMT_1 (A,C,E) or hMT_2 (B,D) melatonin receptors. Membranes were incubated with 2-[^{125}I]-iodomelatonin (■ = 30 pM, △ = 100 pM, ▼ = 300 pM, ◇ = 600 pM, ● = 1000 pM, ▲ = 1400) and control, melatonin (A,B; 10 pM – 1 μM) or luzindole (C-E; 1 nM-100 μM) in active (A-D) and resting buffer (E; + 100 μM GTP, 1 mM $EDTA.Na_2$, 150 mM NaCl). Points shown are the mean from representative experiments independently repeated three times. See Table S1 for derived binding constants (K_B) and cooperativity factors (α; α < 0.01, orthosteric; α ≥ 0.01, allosteric).

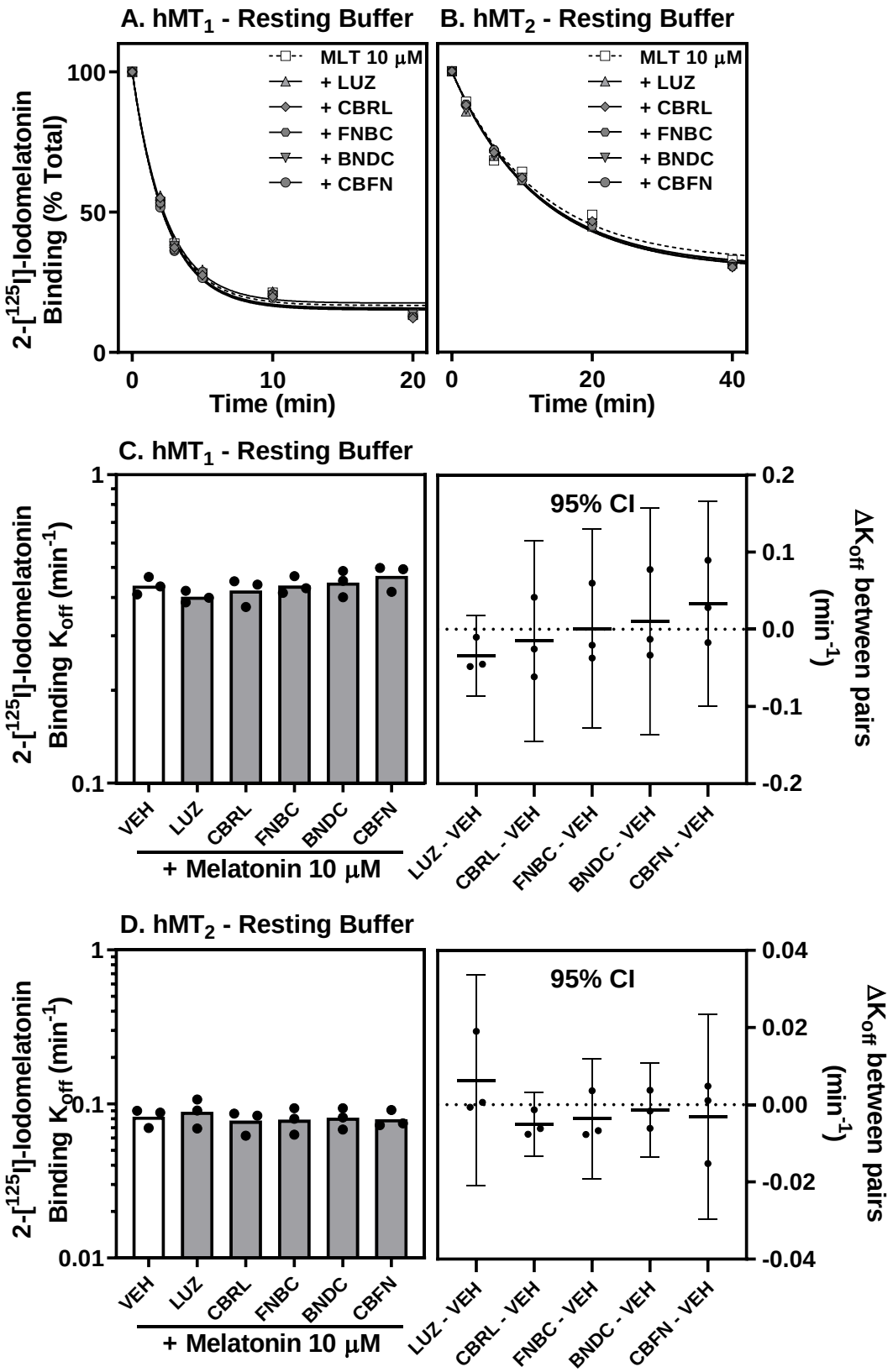
A. hMT1 - Resting Buffer
B. hMT2 - Resting Buffer
MLT 10 µM
+ LUZ
+ CBRL
+ FNBC
+ BNDC
+ CBFN
2-[125I]-Iodomelatonin Binding (% Total)
Time (min)
C. hMT1 - Resting Buffer
D. hMT2 - Resting Buffer
2-[125I]-Iodomelatonin Binding Koff (min-1)
ΔKoff between pairs (min-1)
95% CI
VEH
LUZ
CBRL
FNBC
BNDC
CBFN
+ Melatonin 10 µM
LUZ - VEH
CBRL - VEH
FNBC - VEH
BNDC - VEH
CBFN - VEH

Supplemental Figure 3. Cluster 1-carbamate insecticides likely bind to melatonin receptor orthosteric sites. 2-[^{125}I]-iodomelatonin (100 pM) binding to CHO-hMT$_1$ (A,C) or CHO-hMT$_2$ (B,D) membranes, in resting buffer (100 µM GTP, 1 mM EDTA.Na$_2$, 150 mM NaCl), is allowed to reach equilibrium and dissociation is initiated by challenge with 10 µM melatonin in the absence or the presence of 100 µM luzindole (LUZ), carbaryl (CBRL), fenobucarb (FNBC), bendiocarb (BNDC), or carbofuran (CBFN). (A,B) The ordinate represents 2-[^{125}I]-iodomelatonin binding expressed as percent total 2-[^{125}I]-iodomelatonin binding and the abscissa represents time after concurrent addition of melatonin and test compound. Symbols shown are the mean from three independent experiments, each run in duplicates. (C,D) Symbols on the left panels are means of K_{off} from technical replicates run in duplicate while bars represent the mean of these values (n = 3). Symbols on the right panels indicate the difference (Δ) in 2-[^{125}I]-iodomelatonin K_{off} for individually paired determinations with vehicle or test compounds. The mean ΔK_{off} and 95% confidence intervals are reported on the right as well. See Table S2 for dissociation rates. K_{off} values with test compounds are compared to vehicle using a Friedman test (A: $P = 0.043$; B: $P = 0.74$) with Dunn's post-test for multiple comparisons ($P > 0.05$ for all comparisons).

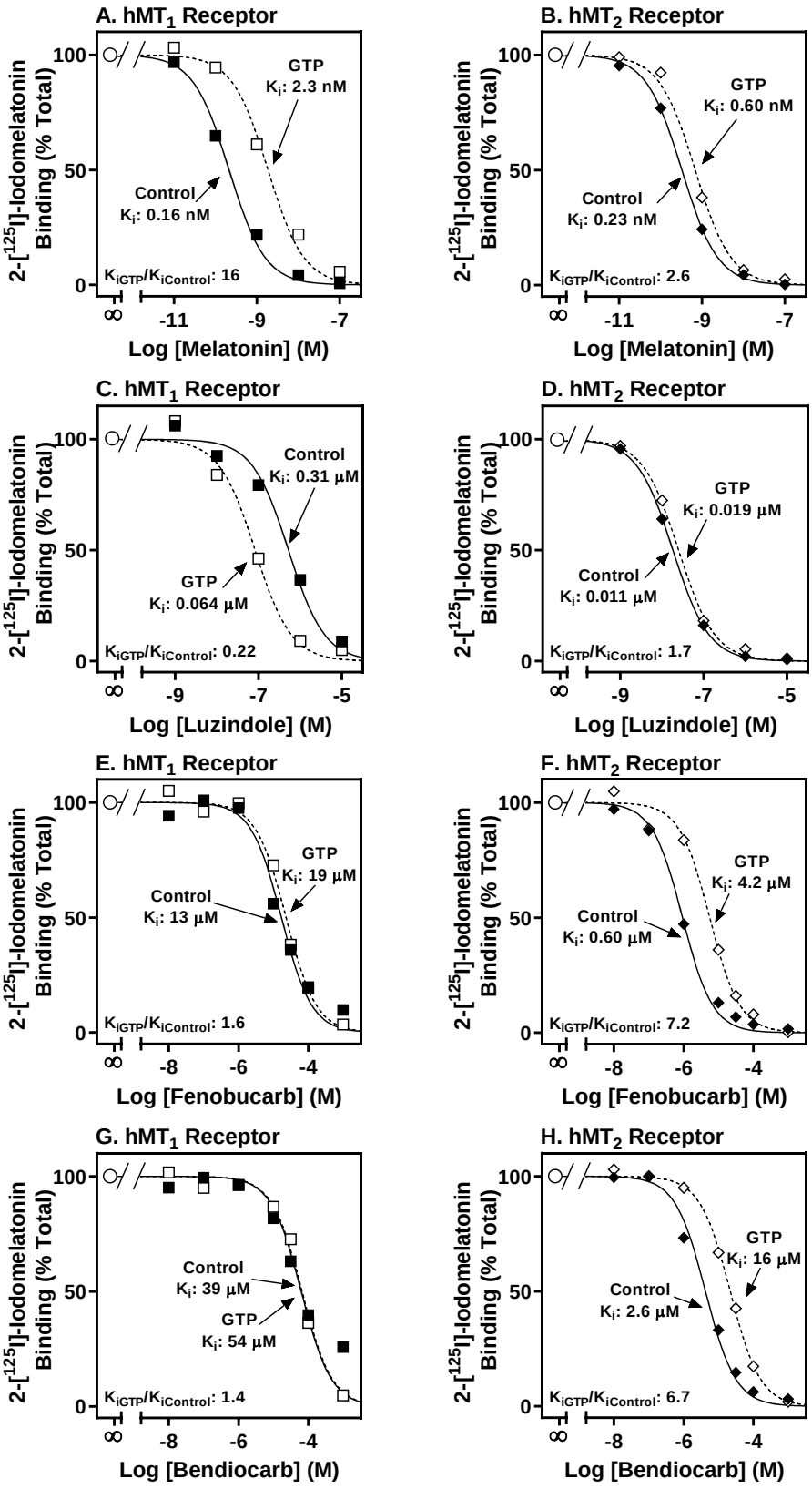
A. hMT1 Receptor
GTP
Ki: 2.3 nM
Control
Ki: 0.16 nM
KiGTP/KiControl: 16
2-[125I]-Iodomelatonin Binding (% Total)
Log [Melatonin] (M)
B. hMT2 Receptor
GTP
Ki: 0.60 nM
Control
Ki: 0.23 nM
KiGTP/KiControl: 2.6
Log [Melatonin] (M)
C. hMT1 Receptor
Control
Ki: 0.31 µM
GTP
Ki: 0.064 µM
KiGTP/KiControl: 0.22
Log [Luzindole] (M)
D. hMT2 Receptor
GTP
Ki: 0.019 µM
Control
Ki: 0.011 µM
KiGTP/KiControl: 1.7
Log [Luzindole] (M)
E. hMT1 Receptor
GTP
Ki: 19 µM
Control
Ki: 13 µM
KiGTP/KiControl: 1.6
Log [Fenobucarb] (M)
F. hMT2 Receptor
GTP
Ki: 4.2 µM
Control
Ki: 0.60 µM
KiGTP/KiControl: 7.2
Log [Fenobucarb] (M)
G. hMT1 Receptor
Control
Ki: 39 µM
GTP
Ki: 54 µM
KiGTP/KiControl: 1.4
Log [Bendiocarb] (M)
H. hMT2 Receptor
GTP
Ki: 16 µM
Control
Ki: 2.6 µM
KiGTP/KiControl: 6.7
Log [Bendiocarb] (M)

Supplemental Figure 4. Carbamate insecticides compete for 2-[^{125}I]-iodomelatonin binding to hMT_1 and hMT_2 melatonin receptors without and with G protein inactivation: Representative Curves. The ordinate represents 2-[^{125}I]-iodomelatonin binding expressed as percent total binding. Membranes from CHO cells stably expressing hMT_1 (A,C,E,G, ■ for control, □ for 100 μM GTP) or hMT_2 (B,D,F,H, ◆ for control, ◇ for 100 μM GTP) melatonin receptors were incubated with 2-[^{125}I]-iodomelatonin (75 pM) in the absence (○) and the presence of various concentrations of melatonin (A,B), luzindole (C,D), fenobucarb (E,F) or bendiocarb (G,H). Points shown are the mean from representative experiments independently repeated at least three times. See Table 3 for derived affinity constants.

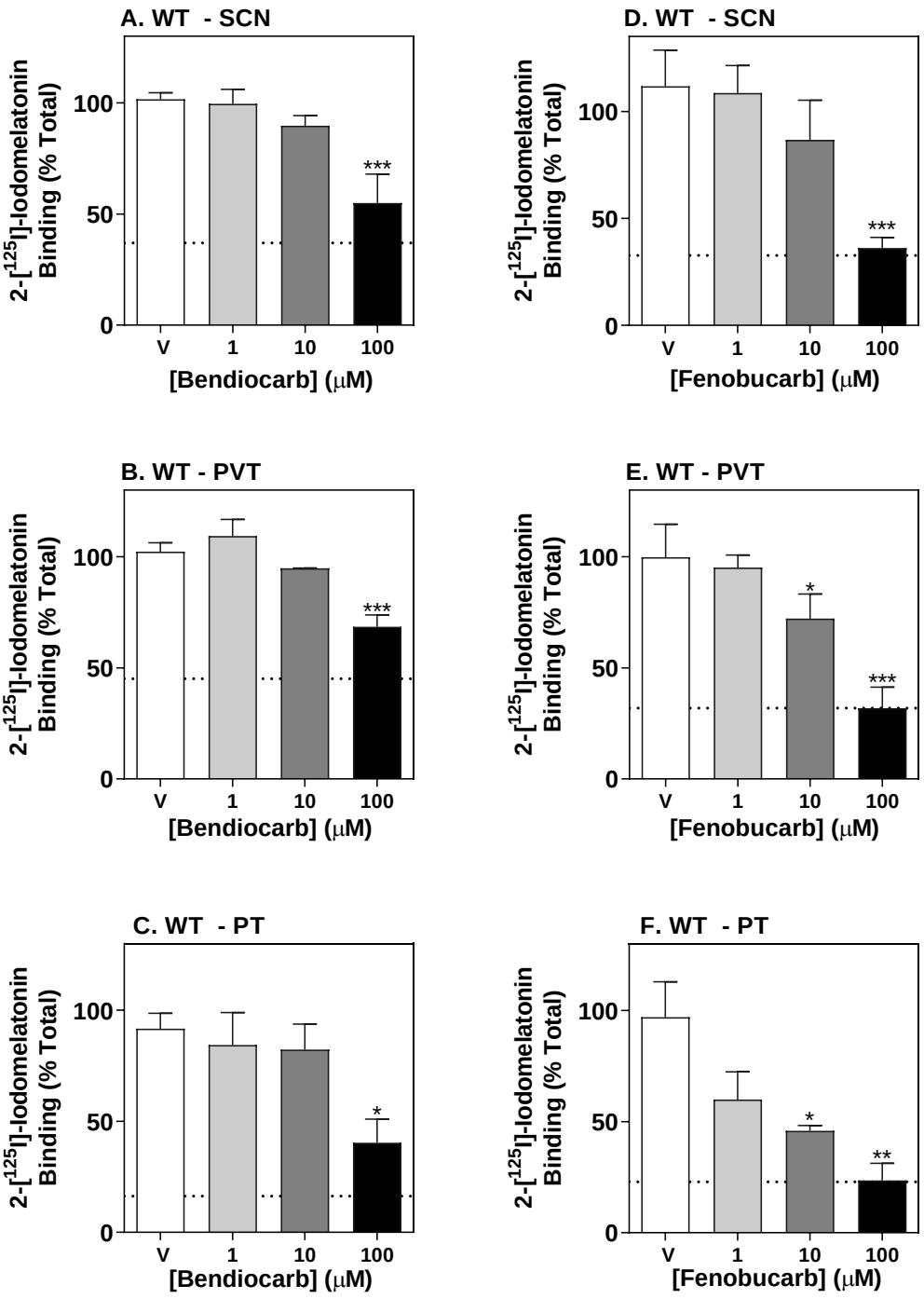

Supplemental Figure 5. Quantitative receptor autoradiography demonstrates bendiocarb and fenobucarb competes *in-vitro* for 2-[^{125}I]-iodomelatonin binding at

melatonin receptors in slices containing the SCN, PVT, and PT from C3H/HeN mice. (A-F) Optical densities obtained for each treatment are normalized to proportion total binding in the absence of drug treatment (bendiocarb A-C, fenobucarb D-F) for each animal. Brain slices were treated with vehicle or drug (1, 10, 100 μM) in vehicle during a 1-hour incubation to determine competition for 2-[^{125}I]-iodomelatonin binding (75 pM) at melatonin receptors in slices containing the SCN, PVT, and PT. Dotted lines in each panel represent non-specific binding for adjacent slices treated with 1 μM melatonin for each data set. Values (n = 2-3) in each panel are compared to % total binding of vehicle using a one-way ANOVA with Dunnet's post-test ($P < 0.05$). *$P < 0.05$; **$P < 0.01$; ***$P < 0.001$. See Table 2 for derived affinity constants. See Supplemental Table 4 for additional information regarding descriptive statistics and data comparisons.